AD-A099 811 NAVAL UNDERWATER SYSTEMS CENTER NEW LONDON CT NEW LO--ETC F/6 12/1
PROBABILITY DISTRIBUTION OF ARRAY RESPONSE FOR RANDOMLY PERTURB--ETC(U)
MAY 81 A H NUTTALL
UNCLASSIFIED NUSC-TR-5687A NL

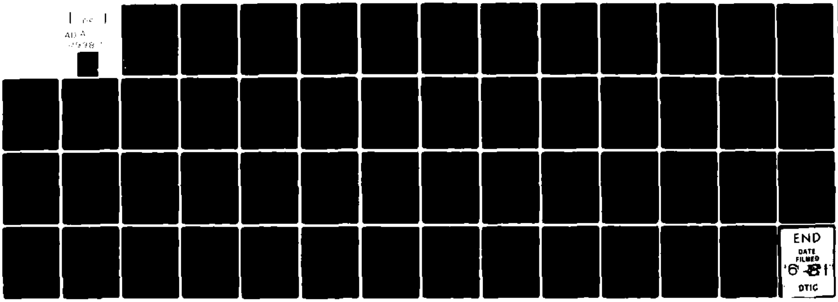

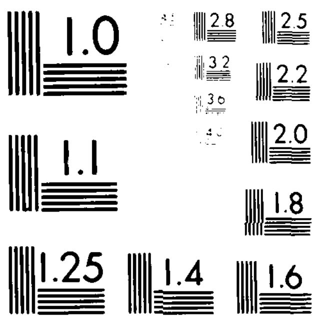

MICROCOPY RESOLUTION TEST CHART

LEVEL II

12

9

NUSC Technical Report 5687A

11

2[illegible] May [illegible]81

14) NUSC-TR-5687A

12 52

6

Probability Distribution of Array Response for Randomly Perturbed Element Gains.

10

Albert H. Nuttall
Surface Ship Sonar Department

Naval Underwater Systems Center
Newport, Rhode Island / New London, Connecticut

Preface

This research was conducted under NUSC Project No. A-752-05, Subproject No. ZR0000101, "Applications of Statistical Communication Theory to Acoustic Signal Processing," Principal Investigator, Dr. A. H. Nuttall (Code 3302), Program Manager, CAPT. David F. Parrish, Naval Material Command (MAT 08L).

The Technical Reviewer for this report was Dr. W. Strawderman (Code 323).

The author benefited from several discussions with Dr. W. Strawderman (Code 323) during the progress of this investigation

Reviewed and Approved: 20 May 1981

D. Walters

D. Walters
Head, Surface Ship Sonar Department

The author of this report is located at the
New London Laboratory, Naval Underwater Systems Center,
New London, Connecticut 06320.

REPORT DOCUMENTATION PAGE		READ INSTRUCTIONS BEFORE COMPLETING FORM
1. REPORT NUMBER TR 5687A	2. GOVT ACCESSION NO. AD-A099 811	3. RECIPIENT'S CATALOG NUMBER
4. TITLE (and Subtitle) PROBABILITY DISTRIBUTION OF ARRAY RESPONSE FOR RANDOMLY PERTURBED ELEMENT GAINS		5. TYPE OF REPORT & PERIOD COVERED 6. PERFORMING ORG. REPORT NUMBER
7. AUTHOR(s) Albert H. Nuttall		8. CONTRACT OR GRANT NUMBER(s)
9. PERFORMING ORGANIZATION NAME AND ADDRESS Naval Underwater Systems Center New London Laboratory New London, CT 06320		10. PROGRAM ELEMENT, PROJECT, TASK AREA & WORK UNIT NUMBERS A-752-05
11. CONTROLLING OFFICE NAME AND ADDRESS Naval Sea Systems Command NAVSEA 06H2 Washington, DC 20362		12. REPORT DATE 20 May 1981 13. NUMBER OF PAGES 48
14. MONITORING AGENCY NAME & ADDRESS(if different from Controlling Office)		15. SECURITY CLASS. (of this report) UNCLASSIFIED 15a. DECLASSIFICATION/DOWNGRADING SCHEDULE

16. DISTRIBUTION STATEMENT (of this Report)

Approved for public release; distribution unlimited.

17. DISTRIBUTION STATEMENT (of the abstract entered in Block 20, if different from Report)

18. SUPPLEMENTARY NOTES

19. KEY WORDS (Continue on reverse side if necessary and identify by block number)

Array Response	Hanning Weighting	Variance of Response
Average Response	Perturbed Element Gains	Volume Array
Characteristic Function	Probability Distribution	
Dolph-Chebyshev Weighting	Side Lobe Levels	
Element Sensitivity	Side Lobe Statistics	

20. ABSTRACT (Continue on reverse side if necessary and identify by block number)

The characteristic function of the power response of an array subject to Gaussian perturbations in its element gains is derived. From this expression, the cumulants are derived, and the mean and standard deviation are plotted for a wide variety of arrays and weights, including linear arrays or planar arrays, and Dolph-Chebyshev, Hanning, or uniform weights. Rules of thumb for the average attainable deep side lobe level and its variation are presented. Expressions for non-Gaussian element perturbations are also derived.

DD FORM 1 JAN 73 1473

TABLE OF CONTENTS

LIST OF ILLUSTRATIONS

LIST OF SYMBOLS

θ	Azimuthal angle of plane-wave arrival
ϕ	Polar angle of plane-wave arrival
c	Speed of propagation
$\tau_k(\theta, \phi)$	Time delay to k-th receiving element
θ_ℓ, ϕ_ℓ	Look direction of beamformer
t	Time
$s(t)$	Waveform received at origin
w_k	k-th beamformer weight
f	Frequency
A	Voltage transfer function of beamformer
d	Separation distance in equi-spaced line array
u,v	Dimensionless variable ((14), (22))
$w_m^{(x)}, w_n^{(y)}$	Weight in m-th (n-th) location of x- (and y-) dimensions
d_x, d_y	Separation distances for planar equi-spaced array
r_k	Relative variation of k-th element voltage gain
$\tilde{A}$	Modified (perturbed) transfer function of beamformer
$\sigma_{k\ell}^2$	Covariance of r_k and r_ℓ
$\tilde{P}$	Perturbed power transfer function of beamformer
$f(\xi)$	Characteristic function of $\tilde{P}$
D, S	Parameters of average array response (27)
$E\{x\}$	Expected (mean) value of x
$Var\{x\}$	Variance of x
σ_r^2	Variance of $\{r_k\}$
m_n	n-th moment of $\{r_k\}$
M	Number of elements in x-dimension of array (= $2M_o + 1$)
N	Number of elements in y-dimension of array (= $2N_o + 1$)
A_r, S_r	Auxiliary real functions ((37))
m	Mean of random power response $\tilde{P}$
σ	Standard deviation of random power response $\tilde{P}$
M_{eff}, N_{eff}, K_{eff}	Effective number of elements ((44), (57), (65))

PROBABILITY DISTRIBUTION OF ARRAY RESPONSE FOR RANDOMLY PERTURBED ELEMENT GAINS

INTRODUCTION

Although an array beamformer with fixed element positions may be designed for good side lobes or skirt selectivity behavior by choice of the element weights, the actual array will undergo degradations due to, e.g., element position movement, element gain quantization, random element gains, etc. Here we will investigate the effect of randomly perturbed element gains, each with omnidirectional response, on the power response of the array beamformer for a single-frequency plane-wave arrival. (We do not consider the effects of random phase shifts.) Since the power response to a single-frequency plane wave is itself then a random variable at each angle of look, we will evaluate its mean and variance as a function of the element locations, the look angle, and the plane-wave arrival frequency, propagation speed, and direction. More generally, we will evaluate the characteristic function of the random power response.* From these results, we will be able to make quantitative statements as to the required tolerance on the individual element gains for a specified side lobe level, as a function of the number of elements and their weight structure.

GENERAL ARRAY CONSIDERATIONS

The geometry to be utilized here is illustrated in figure 1.

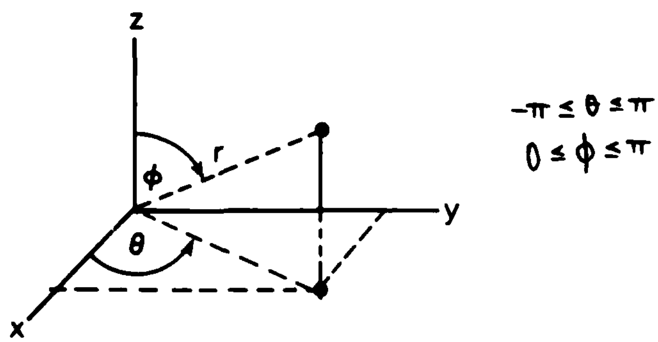

Figure 1. Geometry

---

*Although not pursued here, a single numerical Fourier transformation would then yield the probability distribution of the power response at the particular look direction, arrival angle, etc., of interest.

The radial vector to the location of the k-th element of an arbitrary array (numbered in any convenient fashion) is

$$\vec{v}_k = x_k \vec{i} + y_k \vec{j} + z_k \vec{k}$$

$$= r_k \sin\phi_k \left(\cos\theta_k \vec{i} + \sin\theta_k \vec{j}\right) + r_k \cos\phi_k \vec{k}, \tag{1}$$

where $\vec{i}, \vec{j}, \vec{k}$ are unit vectors in the directors of the x, y, z axes, respectively. The arrival direction vector of a plane wave from direction (θ, ϕ) is

$$\vec{u} = \sin\phi \left(\cos\theta \vec{i} + \sin\theta \vec{j}\right) + \cos\phi \vec{k}. \tag{2}$$

If we adopt the convention that the time delay is zero for the plane wave to reach the origin in figure 1, then the time delay to the k-th element is (for speed of propagation c)

$$-\frac{1}{c}\vec{u}\cdot\vec{v}_k = -\frac{1}{c}\left[x_k \cos\theta \sin\phi + y_k \sin\theta \sin\phi + z_k \cos\phi\right] \equiv -\tau_k(\theta, \phi). \tag{3}$$

Also, if the look direction of the array beamformer is θ_ℓ, ϕ_ℓ, then the delay employed in the k-th receiver element (to accomplish maximum response when steered in the arrival direction) is

$$\tau_k(\theta_\ell, \phi_\ell) = \frac{1}{c}\left[x_k \cos\theta_\ell \sin\phi_\ell + y_k \sin\theta_\ell \sin\phi_\ell + z_k \cos\phi_\ell\right]. \tag{4}$$

If the plane wave arrival is characterized by the waveform s(t) at the origin in figure 1, then the waveform at the output of the delay element in the k-th receiver channel is

$$s\left[t + \tau_k(\theta, \phi) - \tau_k(\theta_\ell, \phi_\ell)\right]. \tag{5}$$

For a beamformer that weights this k-th waveform by w_k and sums over the available element outputs, the voltage transfer function at frequency f of the beamformer (as applied to the plane-wave waveform $s(t)$) is

$$A(f, \theta, \phi, \theta_\ell, \phi_\ell) = \sum_k w_k \exp\left[-i 2\pi f \left\{\tau_k(\theta_\ell, \phi_\ell) - \tau_k(\theta, \phi)\right\}\right]. \tag{6}$$

This is a general expression for the voltage transfer function of the beamformer of an arbitrary volume array. We will adopt an abbreviated version of (6) for later notational convenience:

$$A = \sum_k V_k \,, \tag{7}$$

where

$$V_k = W_k \exp\left[-i\,2\pi f\left\{\tau_k(\theta_\ell, \phi_\ell) - \tau_k(\theta, \phi)\right\}\right] \tag{8}$$

is a deterministic complex function of angles $\theta, \phi, \theta_\ell, \phi_\ell$, frequency f, and element positions $\{x_k, y_k, z_k\}$.

LINEAR ARRAY

The transfer function in (6) applies for an arbitrary array. In the special case of a linear array, we set (see figure 1)

$$x_k = y_k = 0, \tag{9}$$

thereby obtaining

$$\tau_k(\theta, \phi) = \frac{z_k}{c}\cos\phi \tag{10}$$

and

$$V_k = W_k \exp\left[-i\,2\pi f \frac{z_k}{c}\left(\cos\phi_\ell - \cos\phi\right)\right]. \tag{11}$$

Broadside arrivals correspond to $\phi = \pi/2$.

For the further specialization of an equi-spaced line array of spacing d, we let

$$z_k = k\,d, \tag{12}$$

obtaining

$$V_k = W_k \exp(-iku), \tag{13}$$

where dimensionless variable

$$u = 2\pi f \frac{d}{c}\left(\cos\phi_\ell - \cos\phi\right). \tag{14}$$

Then voltage transfer function (7), for this special case, becomes

$$A = \sum_{k} w_k \exp(-iku). \tag{15}$$

Since exp(-iku) has period 2π, there is no need to investigate A outside the range $(-\pi, \pi)$ of u. This range will cover all possible cases of element spacing, look direction, plane-wave arrival angle, frequency, and speed.

PLANAR ARRAY

In the special case of a planar array, we place the array in the x-y plane by setting $z_k = 0$; see figure 1. Also, we limit consideration to a planar array with a grid structure; see figure 2. That is,

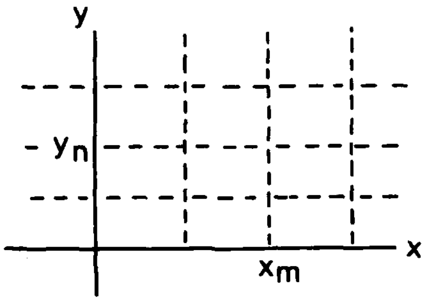

Figure 2. Grid Structure of Planar Array

at each and every x-coordinate x_m, the y-coordinates of the element positions are $\{y_n\}$; the spacing need not be uniform in either coordinate direction. Using a more appropriate labeling system, we express (7) as

$$A = \sum_{m} \sum_{n} v_{mn} , \tag{16}$$

where (from (3) and (8))

$$\tau_{mn}(\theta, \phi) = \frac{1}{c} \sin\phi \left[x_m \cos\theta + y_n \sin\theta \right] \tag{17}$$

and

$$v_{mn} = w_{mn} \exp\left[-i 2\pi f \left\{ \tau_{mn}(\theta_\ell, \phi_\ell) - \tau_{mn}(\theta, \phi) \right\}\right]$$

$$= w_{mn} \exp\left[-i 2\pi f \left\{ \frac{x_m}{c}\left(\sin\phi_\ell \cos\theta_\ell - \sin\phi \cos\theta\right) + \frac{y_n}{c}\left(\sin\phi_\ell \sin\theta_\ell - \sin\phi \sin\theta\right)\right\}\right]. \tag{18}$$

For the further specialization where the weights are obtained via a multiplicative pattern,

$$W_{mn} = W_m^{(x)} W_n^{(y)}, \tag{19}$$

and (16)-(18) yield the voltage transfer function as

$$A = \sum_m W_m^{(x)} \exp\left[-i2\pi f \frac{x_m}{c}\left(\sin\phi_\ell \cos\theta_\ell - \sin\phi \cos\theta\right)\right] \cdot$$
$$\sum_n W_n^{(y)} \exp\left[-i2\pi f \frac{y_n}{c}\left(\sin\phi_\ell \sin\theta_\ell - \sin\phi \sin\theta\right)\right] \equiv \sum_m V_m^{(x)} \sum_n V_n^{(y)}. \tag{20}$$

Thus the transfer function in this case can be represented as the product of two component responses. If weights $\{w_m^{(x)}\}$ are chosen such that the first component in (20) has good side lobe behavior, and weights $\{w_n^{(y)}\}$ are similarly chosen for the second component in (20), then response A will have good side lobe behavior for all look and arrival angles.

Finally, when the elements are equally spaced by d_x in the x-direction and by d_y in the y-direction, (20) yields for the voltage transfer function,

$$A = \sum_m W_m^{(x)} \exp(-imu) \cdot \sum_n W_n^{(y)} \exp(-inv), \tag{21}$$

where dimensionless variables

$$u \equiv 2\pi f \frac{d_x}{c}\left(\sin\phi_\ell \cos\theta_\ell - \sin\phi \cos\theta\right),$$
$$v \equiv 2\pi f \frac{d_y}{c}\left(\sin\phi_\ell \sin\theta_\ell - \sin\phi \sin\theta\right). \tag{22}$$

Since (21) has period 2π in u and v, there is no need to investigate A outside the range $(-\pi, \pi)$ in u and in v.

STATISTICS OF POWER RESPONSE OF ARRAY FOR GAUSSIAN PERTURBATIONS

The general voltage transfer function was given in (7) and (8), where $\{w_k\}$ are the design weights of the array beamformer and are assumed real. However, because of imperfections in manufacture or control, the gains of individual receiving elements are not equal, but are randomly perturbed about their design values. We incorporate this feature in our voltage transfer function (7) by saying that the modified (perturbed) voltage transfer function is

$$\tilde{A} = \sum_k (1 + r_k) v_k \,, \tag{23}$$

where r_k is a (dimensionless) real random variable (with zero mean without loss of generality) that measures the relative perturbation of the k-th element voltage gain. We will assume that $\{r_k\}$ are joint Gaussian with correlation

$$E\{r_k r_\ell\} = \sigma_{k\ell}^2 \,; \tag{24}$$

that is, we allow different elements to have correlated gain perturbations. (Later, the Gaussian assumption will be eliminated in a less complete statistical analysis. Also, even if $\{r_k\}$ are not Gaussian, $\tilde{A}$ will tend toward a complex Gaussian random variable for large numbers of elements, by the Central Limit Theorem. Thus the following results have applicability for a wider range of cases than originally presumed.)

The power transfer function of the perturbed array is

$$\tilde{P} \equiv |\tilde{A}|^2 = \left|\sum_k (1 + r_k) v_k\right|^2 . \tag{25}$$

We are interested in the probability distribution of this real random variable. In appendix A, the distribution is shown to be given by a double integral of a correlated second-order Gaussian density (with unequal variances) over an offset circle. A limited table of this quantity is available in reference 1; however it is not extensive enough for our purposes and it yields little insight into the array behavior. Therefore, instead, we will derive the characteristic function of random variable $\tilde{P}$, and from this quantity extract the cumulants of $\tilde{P}$. The characteristic function of $\tilde{P}$ is derived in appendix B and is given by

$$f(\xi) = E\left\{\exp\left(i\xi\tilde{P}\right)\right\} = \left[1 - i\xi 2D + (i\xi)^2\left(D^2 - |S|^2\right)\right]^{-1/2} \cdot$$

$$\exp\left[i\xi \frac{|A|^2 - i\xi\left(|A|^2 D - \mathrm{Re}\{A^2 S^*\}\right)}{1 - i\xi 2D + (i\xi)^2\left(D^2 - |S|^2\right)}\right] , \tag{26}$$

where A is given by (7) and

$$D = \sum_k \sum_j \sigma_{kj}^2 v_k v_j^* \,,$$

$$S = \sum_k \sum_j \sigma_{kj}^2 v_k v_j \,. \tag{27}$$

Thus the three fundamental functions A, D, and S completely characterize the statistical behavior of $\tilde{P}$. A single numerical Fourier transform of (26) would yield the probability distribution of $\tilde{P}$ for specified values of A, D, and S, if desired; see reference 2.

The cumulants of $\tilde{P}$ are derived from (26) in appendix B; the first three are given by

$$E\{\tilde{P}\} = |A|^2 + D,$$

$$\mathrm{Var}\{\tilde{P}\} = D^2 + |S|^2 + 2D|A|^2 + 2\,\mathrm{Re}\{A^2 S^*\},$$

$$E\{(\tilde{P} - E\{\tilde{P}\})^3\} = 2D^3 + 6D|S|^2 + 6D^2|A|^2 + 6|S|^2|A|^2 + 12D\,\mathrm{Re}\{A^2 S^*\}. \quad (28)$$

The first relationship for the mean $E\{\tilde{P}\}$ actually holds for any distribution of $\{r_k\}$, not just Gaussian; this is most easily seen by direct use of (25), (24), (7), and (A-3).

Two useful special cases of the above results are available from (7) and (27):

$$\left.\begin{aligned} A &= \sum_k v_k \\ D &= \sum_k \sigma_k^2 |v_k|^2 \\ S &= \sum_k \sigma_k^2\, v_k^2 \end{aligned}\right\} \quad \text{uncorrelated perturbations} \quad (29)$$

,

$$\left.\begin{aligned} A &= \sum_k v_k \\ D &= \sigma_r^2 \sum_k |v_k|^2 \\ S &= \sigma_r^2 \sum_k v_k^2 \end{aligned}\right\} \quad \text{uncorrelated equal-variance perturbations} \quad (30)$$

where, in the latter case, σ_r^2 is the common variance of the random gain variable introduced in (23).

STATISTICS FOR NON-GAUSSIAN PERTURBATIONS

In this section, random perturbations $\{r_k\}$ are assumed statistically independent with identical statistics, but are not assumed Gaussian. We let

$$E\{r_k^n\} \equiv m_n \; ; \; m_1 = 0, \; m_2 = \sigma_r^2 . \quad (31)$$

The mean of random power response $\tilde{P}$ is given, by use of (25), (31), and (7), as

$$E\{\tilde{P}\} = \sum_k \sum_j E\{(1+r_k)(1+r_j)\} v_k v_j^* = \sum_k \sum_j (1+\sigma_r^2 \delta_{kj}) v_k v_j^*$$

$$= |A|^2 + \sigma_r^2 \sum_k |v_k|^2 = |A|^2 + m_2 \sum_k |v_k|^2 . \tag{32}$$

The variance of $\tilde{P}$ is derived in appendix C and is given by

$$\mathrm{Var}\{\tilde{P}\} = 2\, m_2 \left[|A|^2 \sum_k |v_k|^2 + \mathrm{Re}\left\{ A^2 \sum_k v_k^{*2} \right\} \right]$$

$$+ 4\, m_3\, \mathrm{Re}\left\{ A \sum_k |v_k|^2 v_k^* \right\}$$

$$+ m_2^2 \left[\left(\sum_k |v_k|^2 \right)^2 + \left| \sum_k v_k^2 \right|^2 \right] + (m_4 - 3m_2^2) \sum_k |v_k|^4 . \tag{33}$$

For Gaussian perturbations, $m_3 = 0$, $m_4 = 3m_2^2$, and (33) reduces to (28), where D and S are given by (30). For a uniform probability density function for $\{r_k\}$, we have

$$m_1 = 0,\ m_2 = \sigma_r^2,\ m_3 = 0,\ m_4 = 1.8\,\sigma_r^4,\ m_n = \frac{(3\sigma_r^2)^{n/2}}{n+1},\ n \text{ even}, \quad \text{(uniform)}, \tag{34A}$$

whereas, for a zero-mean exponential density, we have

$$m_1 = 0,\ m_2 = \sigma_r^2,\ m_3 = 2\sigma_r^3,\ m_4 = 9\sigma_r^4,\ m_n = (-\sigma_r)^n + n\,\sigma_r\, m_{n-1}, \quad \text{(exponential)}. \tag{34B}$$

Generally, when m_3 is zero (as, for example, for a symmetric density for $\{r_k\}$), the only change in the mean and variance of $\tilde{P}$ from the Gaussian results in (28) is the addition of the $m_4 - 3m_2^2$ constant term in (33); the latter two examples, above, indicate that this term can be either positive or negative.

One specification of the relative randomness r_k of the k-th element voltage gain (introduced in (23)) is its variance σ_k^2. However, it is sometimes more useful to express this variation in decibels. This problem

is addressed in appendix D, and results are plotted in figures 3 and 4. For example, from figure 3, for Gaussian perturbations, if $\sigma_k = 0.1$ ($\sigma_k^2 = 0.01$), the range of element gain perturbations is (-1.19, 1.05) dB, with probability 0.9 - 0.1 = 0.8; that is, the element gain is less than -1.19 dB from design 10 percent of the time and greater than 1.05 dB from design 10 percent of the time. Figure 4 gives results for a uniform distribution of element variations; the corresponding range for $\sigma_k = 0.1$ is (-1.30, 1.13) dB, with probability 0.8.

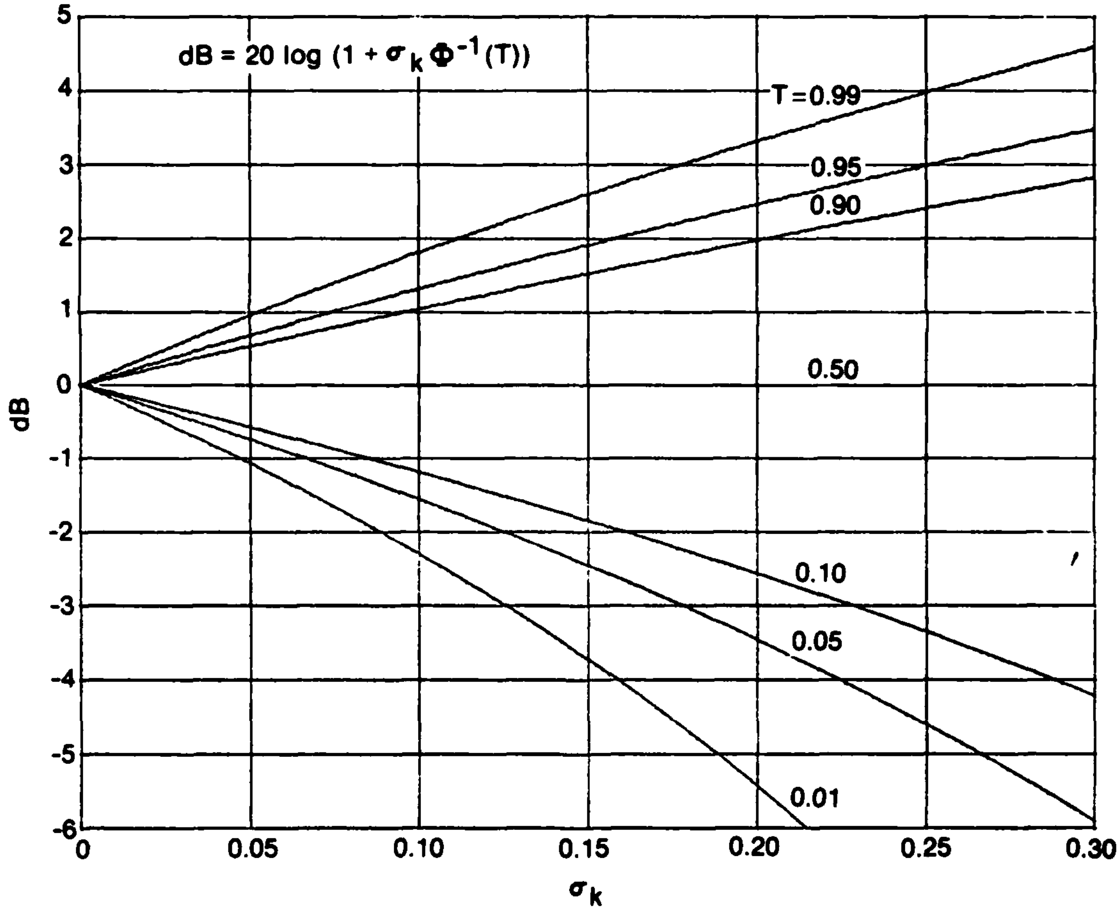

Figure 3. Range of Element Variations for Gaussian Perturbations

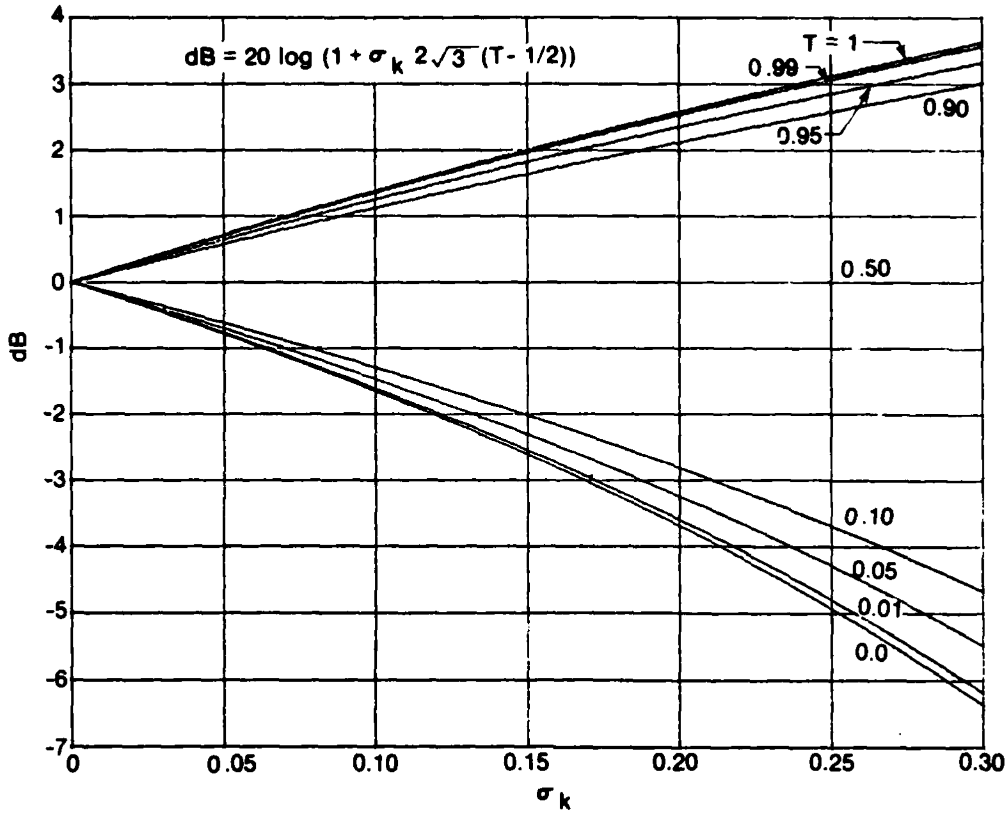

Figure 4. Range of Element Variations for Uniformly Distributed Perturbations

APPLICATIONS TO ARRAYS

When the perturbations $\{r_k\}$ in (25) are not zero, the random pattern assumed by power transfer function $\tilde{P}$ depends on the particular realization of $\{r_k\}$. In figure 5, four different realizations, for a 20 element equi-spaced, equi-weighted line array with $\sigma_r^2 = 0.01$, are plotted for u in the range $(0,\pi)$; see (12)-(14). In figure 6, the element weighting $\{w_k\}$ is changed to Hamming,

$$w_k = 0.54 - 0.46 \cos\left(2\pi \frac{k-1}{K-1}\right), \quad 1 \le k \le K, \tag{35}$$

and the variance σ_r^2 is reduced to 0.001. Although the ideal Hamming response ($r_k = 0$) would continue to decay with u, the four random realizations in figure 6 saturate at a value near -40 dB for this example.

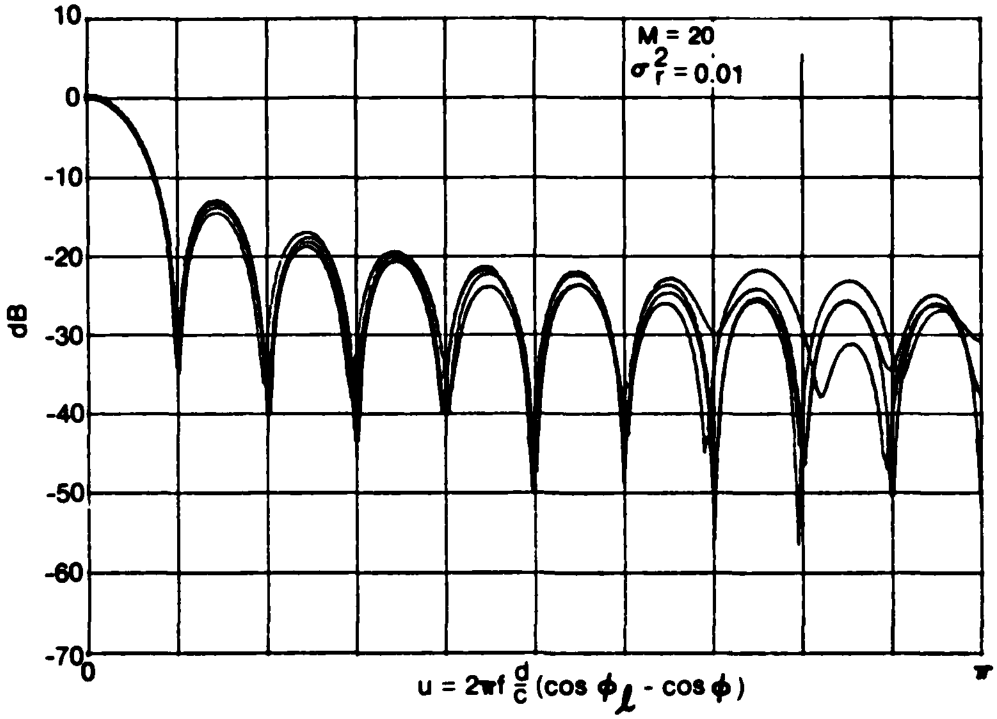

Figure 5. Four Random Power Responses for Line Array, Equi-Weighted

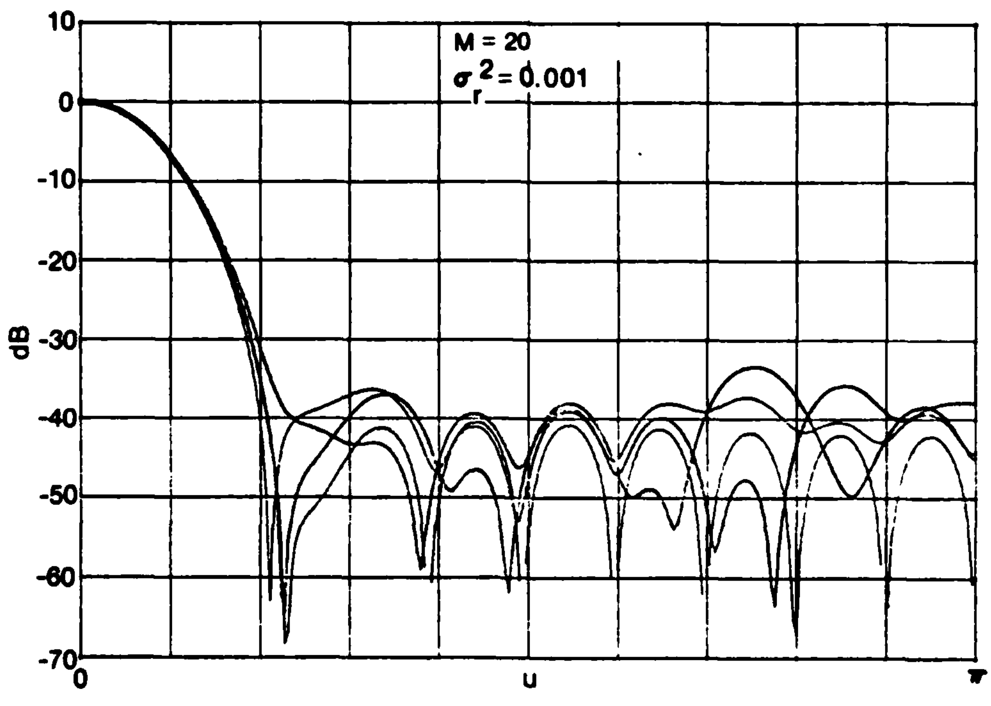

Figure 6. Four Random Power Responses for Line Array, Hamming Weighting

In figure 7, four random power responses of a planar array of 16 x 16 elements, with multiplicative -30 dB Dolph-Chebyshev weighting and σ_r^2 = 0.01, are plotted for v = 0; see (19)-(22). In figure 8, the only change is to set v = u; since, according to (21), the ideal pattern drops to -60 dB along this slice in the u, v plane, the saturation level is lower in this figure than in figure 7.

For both the linear and planar arrays, we wish to find the average and the standard deviation of the random power response as a function of the number of elements, weighting, element gain variation, etc.

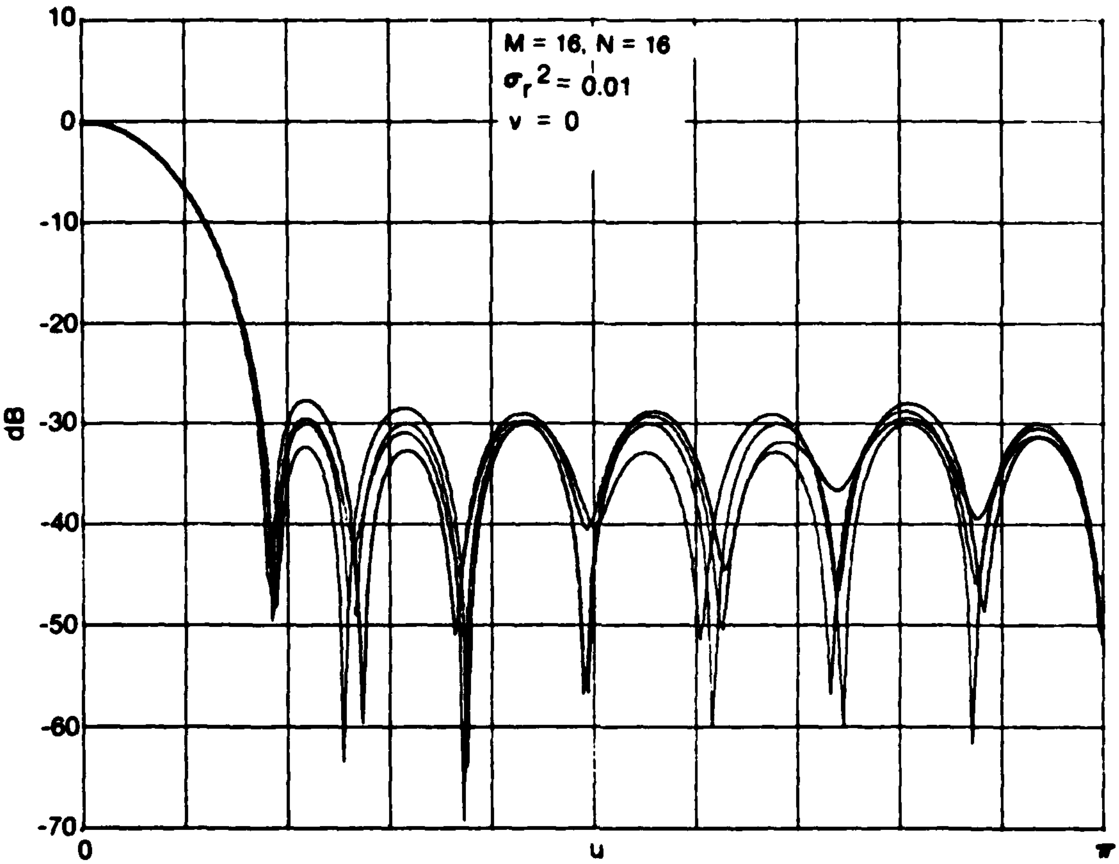

Figure 7. Four Random Power Responses for Planar Array, Dolph-Chebyshev Weighting; v = 0

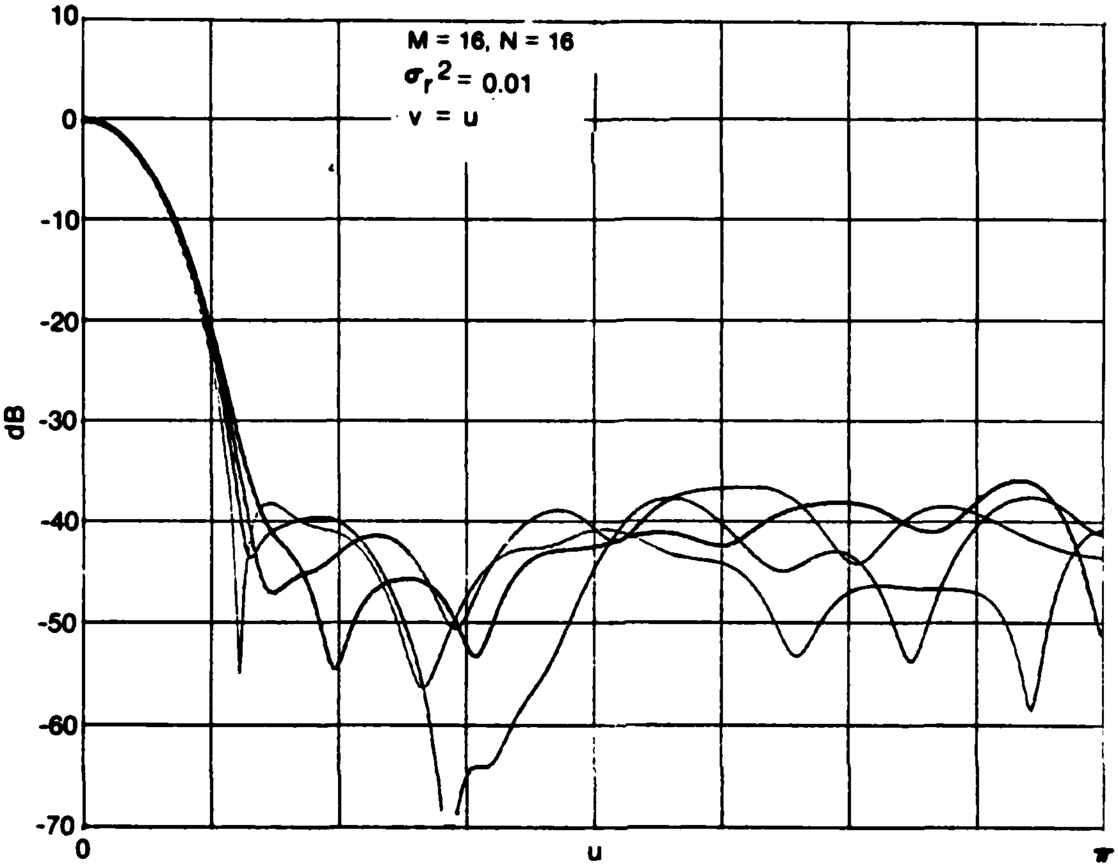

Figure 8. Four Random Power Responses for Planar Array, Dolph-Chebyshev Weighting; v = u

LINEAR ARRAY

We restrict consideration here to uncorrelated and equal-variance gain perturbations, an equi-spaced line array, and symmetric weights. Then (30) and (13)-(14) are relevant to the discussion. We find, for M elements (M even),

$$A = \exp\left(-i\frac{M+1}{2}u\right) A_r(u),$$

$$D = \sigma_r^2 \, S_r(0),$$

$$S = \exp\left(-i(M+1)u\right)\sigma_r^2 \, S_r(u), \tag{36}$$

where real functions

$$A_r(u) \equiv 2\sum_{m=1}^{M/2} w_m \cos\left(\frac{2m-M-1}{2}u\right),$$

$$S_r(u) \equiv 2\sum_{m=1}^{M/2} w_m^2 \cos\left((2m-M-1)u\right). \tag{37}$$

Then (28) yields, for the statistics of the random power pattern $\tilde{P}$,

$$E\{\tilde{P}\} = A_r^2(u) + \sigma_r^2 S_r(0),$$

$$\mathrm{Var}\{\tilde{P}\} = 2\sigma_r^2 A_r^2(u)\left[S_r(0) + S_r(u)\right] + \sigma_r^4\left[S_r^2(0) + S_r^2(u)\right],$$

$$E\left\{\left(\tilde{P} - E\{\tilde{P}\}\right)^3\right\} = 6\,\sigma_r^4 A_r^2(u)\left[S_r(0) + S_r(u)\right]^2 + 2\sigma_r^6 S_r(0)\left[S_r^2(0) + 3S_r^2(u)\right]. \tag{38}$$

Some useful properties of these functions are listed below:

$$A = \sum_k v_k = \sum_{m=1}^{M} w_m \exp(-imu) \equiv A_M(u) = A_M(u+2\pi) = A_M^*(-u),$$

$$S = \sigma_r^2 \sum_k v_k^2 = \sigma_r^2 \sum_{m=1}^{M} w_m^2 \exp(-im2u) \equiv S_M(u) = S_M(u+\pi),$$

$$\sigma_r^2 \frac{1}{2\pi}\int_{2\pi} dv\, A_M(v)\, A_M^*(v-2u) = S_M(u),$$

$$\sigma_r^2 \frac{1}{2\pi}\int_{2\pi} dv\, A_M(v)\, A_M(2u-v) = S_M(u). \tag{39}$$

Thus $A_M(u)$ is periodic of period 2π and possesses conjugate symmetry; $S_M(u)$ has period π; and either the correlation or convolution of $A_M(u)$ yields $S_M(u)$, where 2u appears as the shift in the argument of the correlation or convolution. These properties enable us to limit examination of (38) to the range $(0,\pi)$ in u.

In figure 9, an M = 20 element line array with equal weighting and σ_r^2 = 0.01 is considered. Four curves are drawn in the figure; starting from the bottom up, they correspond to (1) the ideal power pattern, (2) the mean power pattern, (3) the mean plus one standard deviation (Std. Dev.), and (4) the mean plus two standard deviations. Mathematically, these are

$$\begin{aligned} &(1) \quad E\{\tilde{P}\} \text{ for } \sigma_r^2 = 0 \\ &\left.\begin{aligned} &(2) \quad E\{\tilde{P}\} \\ &(3) \quad E\{\tilde{P}\} + \text{Std. Dev.}\{\tilde{P}\} \\ &(4) \quad E\{\tilde{P}\} + 2\,\text{Std. Dev.}\{\tilde{P}\} \end{aligned}\right\} \text{ for } \sigma_r^2 \neq 0. \end{aligned} \tag{40}$$

These curves are labeled m(σ_r^2 = 0), m, m + σ, m + 2σ , respectively. Thus, for u near π, although the mean power response m is only increased by about 1 dB (near the peak), the mean plus two standard deviation response, m + 2σ , is increased by about 4 dB. Probabilistic interpretations and the depth of the attainable levels in the deep side lobe region will be presented later in this subsection.

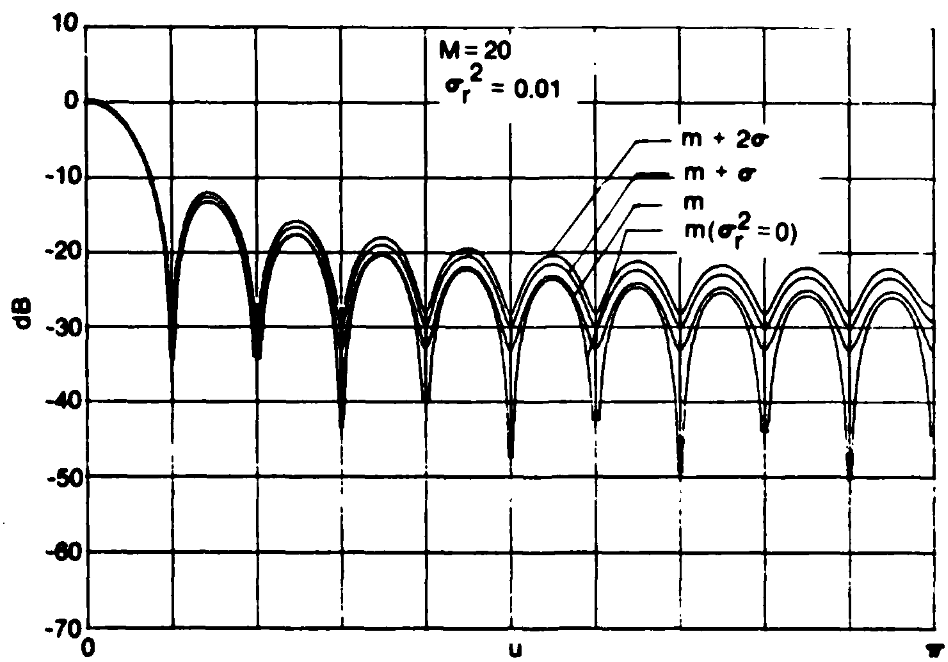

Figure 9. Average Power Responses for Equal Weighting

In figure 10, results for a 20 element array with Hanning weighting are presented; that is,

$$W_m = 1 - \cos\left(\frac{2\pi m}{M+1}\right), \quad 1 \le m \le M. \tag{41}$$

Values of $\sigma_r^2 = 0.01$, 0.001, and 0.0001 are given in figures 10a, 10b, and 10c, respectively. The side lobe level of -30 dB is not attainable for $\sigma_r^2 = 0.01$; whereas, for $\sigma_r^2 = 0.0001$, deep side lobe levels of -45 dB are attainable.

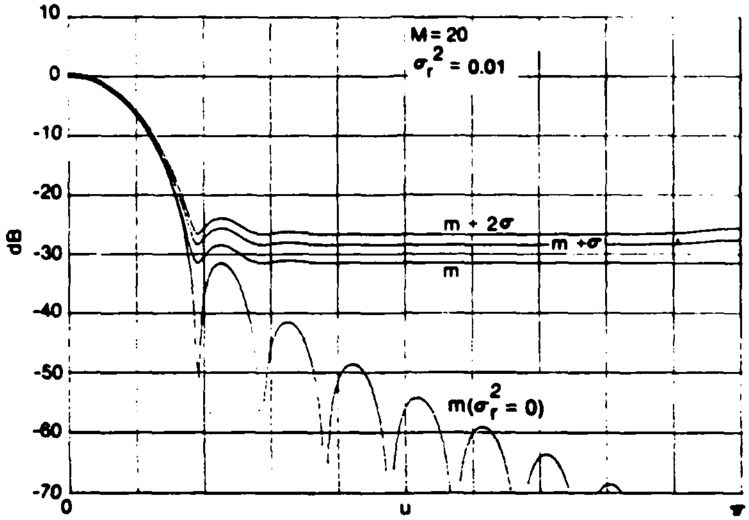

Figure 10a. Average Power Responses for Hanning Weighting; $\sigma_r^2 = 0.01$

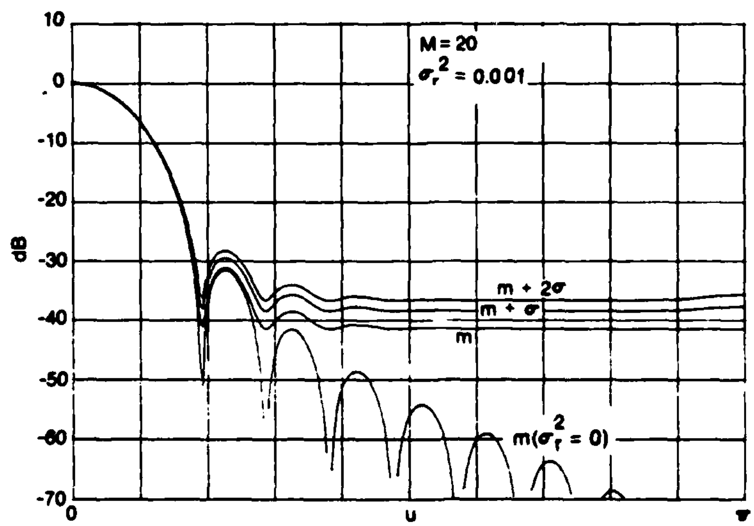

Figure 10b. Average Power Responses for Hanning Weighting; $\sigma_r^2 = 0.001$

Figure 10. Average Power Responses for Hanning Weighting

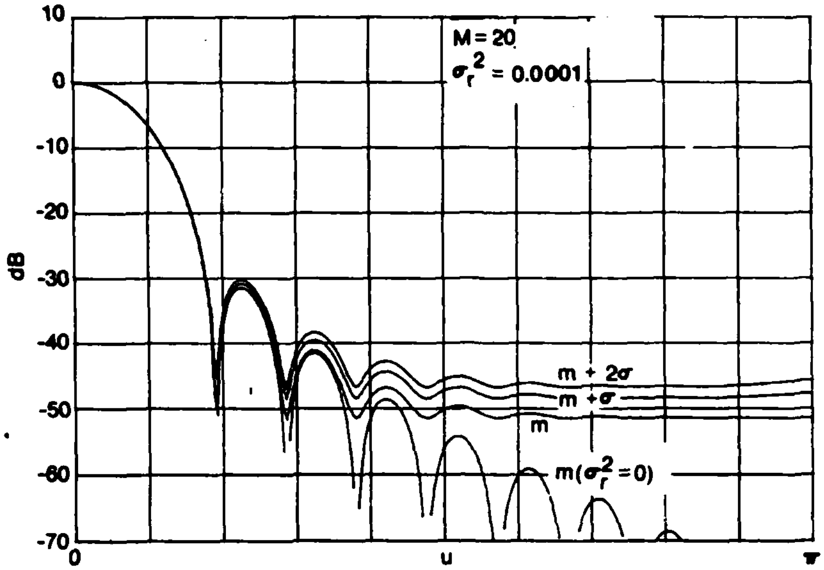

Figure 10c. Average Power Responses for Hanning Weighting; σ_r^2 = 0.0001

Figure 10. (Cont'd) Average Power Responses for Hanning Weighting

In figure 11, the Hamming weighting of (35) is employed. It is seen in figure 11a that σ_r^2 = 0.001 gives about a 7 dB increase in the m + 2σ curve over the ideal response (at the peaks). The results for σ_r^2 = 0.0001 in figure 11b yield approximately a 3 dB increase.

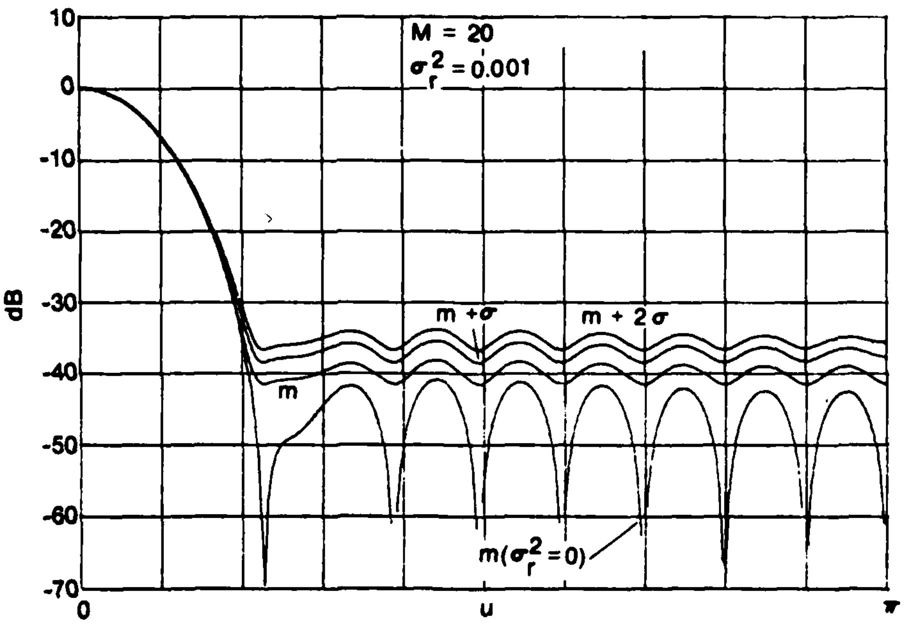

Figure 11a. Average Power Responses for Hamming Weighting; σ_r^2 = 0.001

Figure 11. Average Power Responses for Hamming Weighting

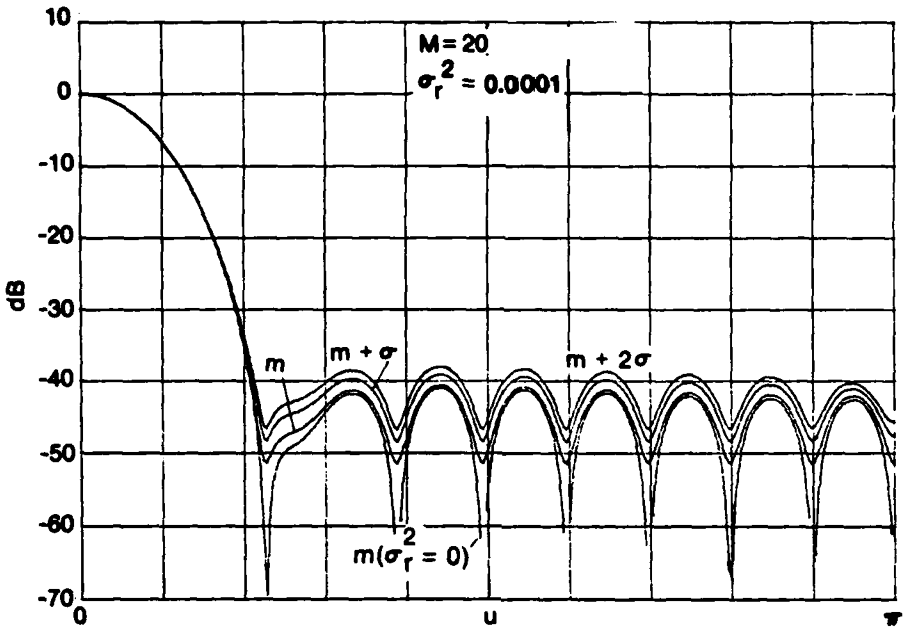

Figure 11b. Average Power Responses for Hamming Weighting; $\sigma_r^2 = 0.0001$

Figure 11. (Cont'd) Average Power Responses for Hamming Weighting

A Dolph-Chebyshev array design (reference 3) is considered in figure 12. This particular case is a 20 element array designed for -20 dB side lobes. Results for $\sigma_r^2 = 0.01$ and 0.001 are presented in figures 12a and 12b, respectively. The only change in figure 13 is that the design is for -30 dB side lobes; it is seen that the value of $\sigma_r^2 = 0.001$ yields a 2.5 dB increase in the m + 2σ curve over the m($\sigma_r^2 = 0$) curve. Finally, in figure 14, the design is for -40 dB side lobes, and $\sigma_r^2 = 0.0001$ is going to be necessary to take advantage of this design.

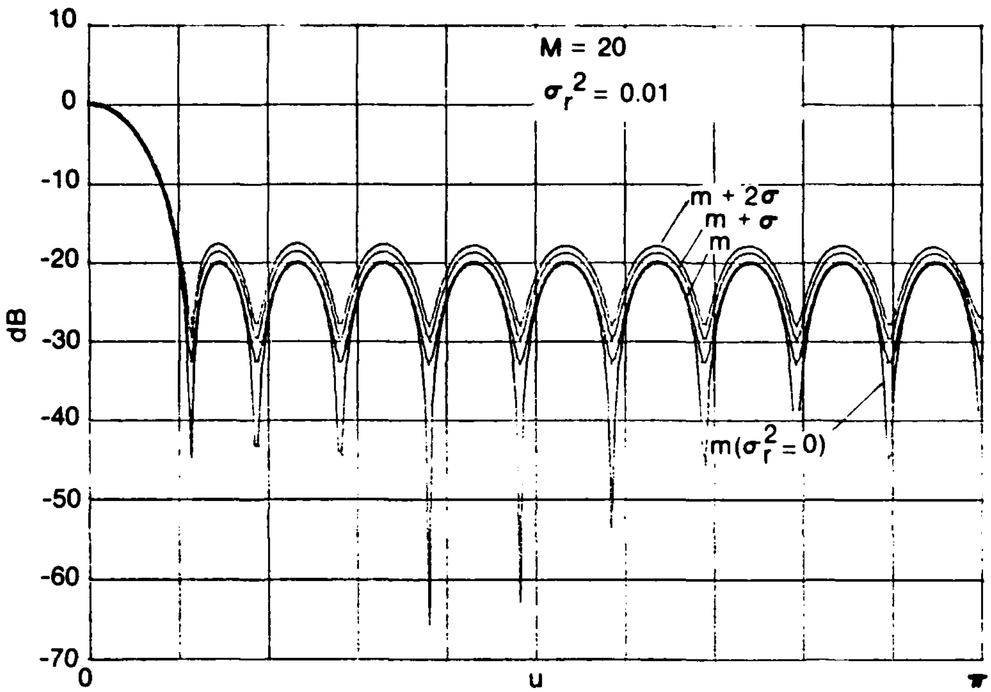

Figure 12a. Average Power Responses for Dolph-Chebyshev -20 dB Weighting; $\sigma_r^2 = 0.01$

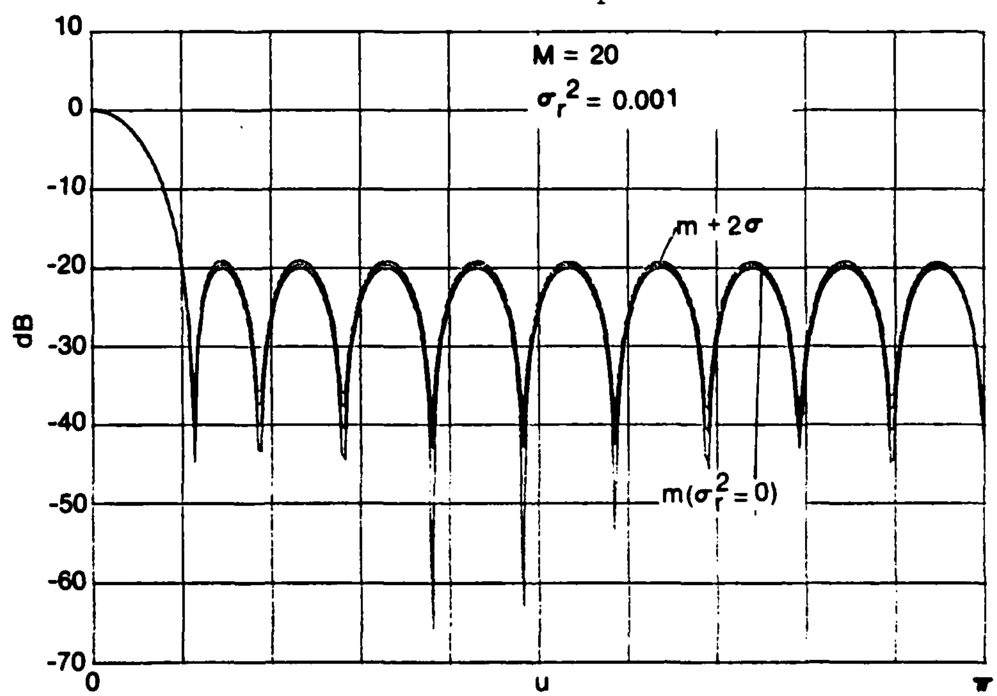

Figure 12b. Average Power Responses for Dolph-Chebyshev -20 dB Weighting; $\sigma_r^2 = 0.001$

Figure 12. Average Power Responses for Dolph-Chebyshev -20 dB Weighting

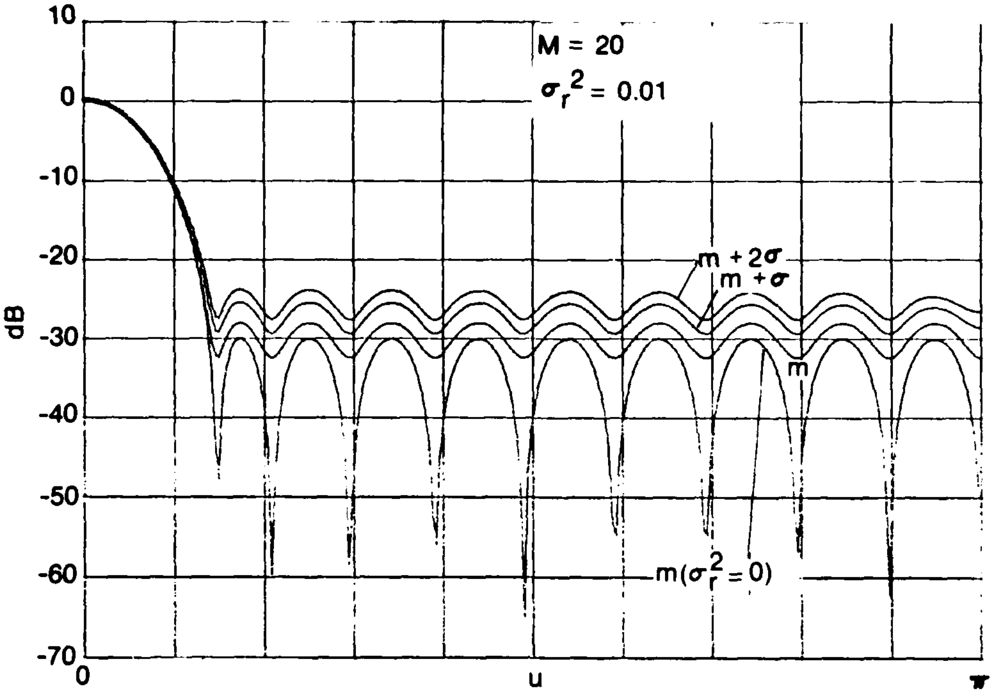

Figure 13a. Average Power Responses for Dolph-Chebyshev -30 dB Weighting; $\sigma_r^2 = 0.01$

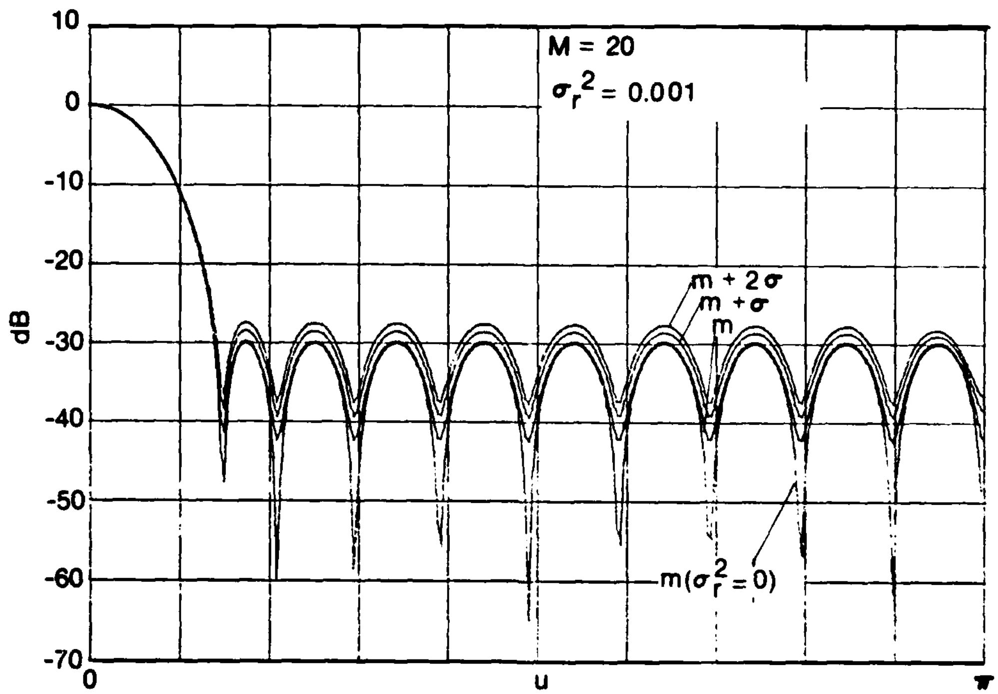

Figure 13b. Average Power Responses for Dolph-Chebyshev -30 dB Weighting; $\sigma_r^2 = 0.001$

Figure 13. Average Power Responses for Dolph-Chebyshev -30 dB Weighting

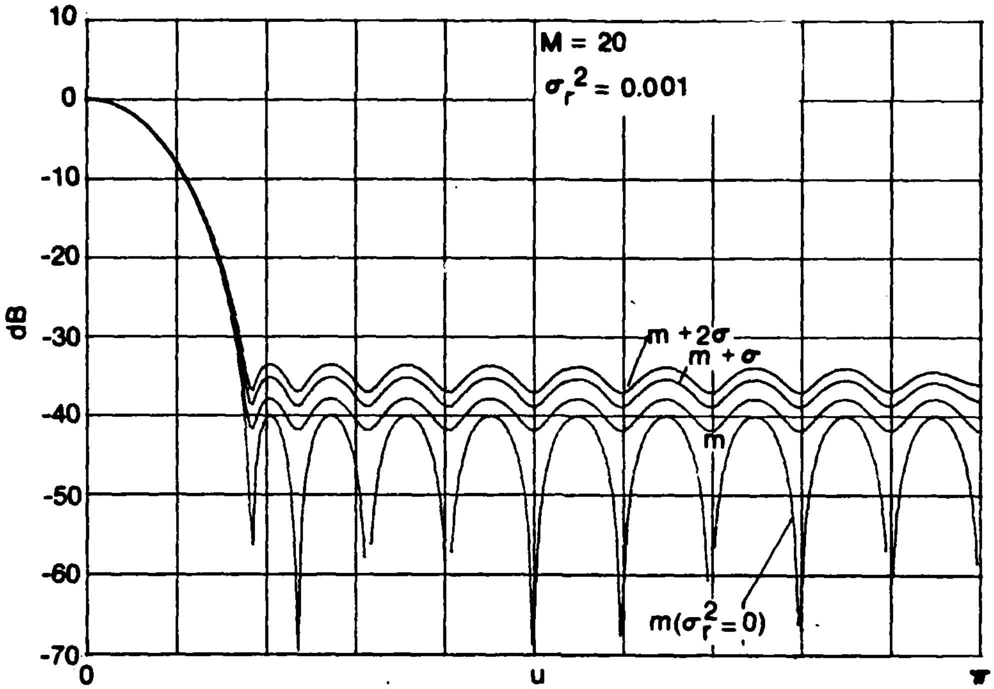

Figure 14a. Average Power Responses for Dolph-Chebyshev -40 dB Weighting; $\sigma_r^2 = 0.001$

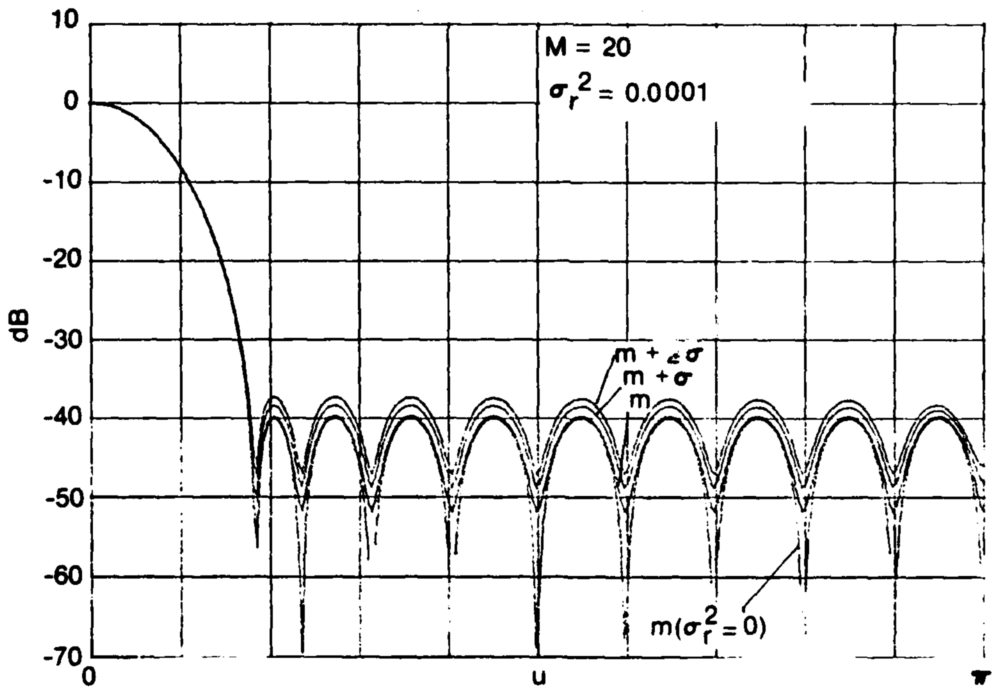

Figure 14b. Average Power Responses for Dolph-Chebyshev -40 dB Weighting; $\sigma_r^2 = 0.0001$

Figure 14. Average Power Responses for Dolph-Chebyshev -40 dB Weighting

In the region where the ideal power pattern response becomes very low (to be called the deep side lobe region), as, for example, in figure 10 for larger u, or in any of the figures for u in a notch, the mean response curves m, m + σ, and m + 2σ saturate and do not drop continuously. It is useful to know these saturation levels and what they depend on, so that design criteria can be developed for future cases. From (36) and (37), we have (for $w_m \geq 0$)

$$|A|^2_{max} = \left(\sum_{m=1}^{M} w_m\right)^2 ,$$

$$D = \sigma_r^2 \sum_{m=1}^{M} w_m^2 . \tag{42}$$

Therefore

$$\frac{D}{|A|^2_{max}} = \frac{\sigma_r^2}{M_{eff}} , \tag{43}$$

where

$$M_{eff} \equiv \frac{\left(\sum_{m=1}^{M} w_m\right)^2}{\sum_{m=1}^{M} w_m^2} . \tag{44}$$

Now in the deep side lobe region, $|A|^2 \ll D$; therefore (28) indicates that the depth of the mean power response is approximately D. Since the curves in figures 9-14 are normalized to 0 dB at their peak for $\sigma_r^2 = 0$, (43) gives the attainable depth of the mean power response relative to the peak. Table 1 gives the values of M_{eff} in (44) for two types of weighting. By Schwartz's inequality, $M_{eff} \leq M$; the upper limit is attainable only for equal weighting.

Table 1. Values of M_{eff}

Weighting	M_{eff}
Equal	M
Hanning	$\frac{M+1}{1.5}$ $(M \geq 2)$

As an example, for equal weighting, M = 20, $\sigma_r^2 = 0.01$, then (43) and table 1 yield

$$\frac{D}{|A|^2_{max}} = \frac{0.01}{20} = 0.0005 = -33 \text{ dB}. \tag{45}$$

This value is seen to be attained at the notches in figure 9. A second example, for Hanning weighting, M = 20, $\sigma_r^2 = 0.001$, yields

$$\frac{D}{|A|^2_{max}} = \frac{0.001}{21/1.5} = -41.5 \text{ dB}. \tag{46}$$

This value can be seen in figure 10b for larger u.

In the deep side lobe region, characterized by $|A|^2 \ll D$, we also have $|S|^2 \ll D^2$, as may be seen from (39) and (42). (This is true except for u near π.) Then (28) yields

$$E\{\tilde{P}\} \cong D, \quad \mathrm{Var}\{\tilde{P}\} \cong D^2. \tag{47}$$

This means that

$$\begin{aligned} m &\cong D, \\ m + \sigma &\cong D + D = 2D, \\ m + 2\sigma &\cong D + 2D = 3D. \end{aligned} \tag{48}$$

That is, in the deep side lobe region, the m + σ curve is 3 dB above the m curve, and the m + 2σ curve is 4.8 dB above the m curve. These results are independent of M, σ_r^2, and the weighting. The behavior predicted by (48) is observed in figures 9-14.

Equation (43), coupled with (48), enables a simple rule-of-thumb for the deep side lobe region. Furthermore, a simple probabilistic interpretation is possible in that region, as follows. When $|A|^2 \ll D$ and $|S|^2 \ll D^2$, (A-4) yields

$$\sigma_x^2 = \sigma_y^2 = \frac{1}{2}D, \quad \rho \cong 0. \tag{49}$$

Then (A-5) and (A-6) yield

$$\mathrm{Prob}(\tilde{P} < L) = 1 - \exp\left(-\frac{L}{D}\right), \quad L > 0. \tag{50}$$

In particular, referring to (48),

$$\mathrm{Prob}\left(\tilde{P} < m + k\sigma\right) = \mathrm{Prob}\left(\tilde{P} < D(1+k)\right) = 1 - \exp(-1-k). \tag{51}$$

A short table follows. It shows that the probability of the random power response being less than its mean m is 0.63, less than $m + \sigma$ with probability 0.86, and less than $m + 2\sigma$ 95 percent of the time.

Table 2. Probabilities of the Random Power Response in Deep Side Lobe Region

k	0	1	2
Prob	0.63	0.86	0.95

The fact that the probability is not 0.5 for k = 0 in (51) is a result of the asymmetry of the probability density function of $\tilde{P}$ in the deep side lobe region; in fact, (50) yields the exponential density function D^{-1} exp $(-\tilde{P}/D)$ for $\tilde{P} \geq 0$. (If $\tilde{P}$ had been Gaussianly distributed, the probabilities in table 2 would be 0.50, 0.84, and 0.98, respectively.)

When the element gain perturbation are not Gaussian, (33) indicates that Var $\{\tilde{P}\}$ is changed. However, for a uniform density, the results in (34) give $m_3 = 0$ and m_4 proportional to σ_r^4. For the small values of σ_r^2 of interest in the array examples in figures 9-14, the curves for the uniform density were virtually indistinguishable and have not been presented.

PLANAR ARRAY

For a planar array, the random gain perturbations change (16) to read

$$\tilde{A} = \sum_m \sum_n (1 + r_{mn}) v_{mn} = A + \sum_m \sum_n r_{mn} v_{mn}, \tag{52}$$

where v_{mn} is given by (18). For a multiplicative weight pattern (19), (18) yields

$$v_{mn} = v_m^{(x)} v_n^{(y)}, \tag{53}$$

where $v_m^{(x)}$ and $v_n^{(y)}$ are given by (20). Thus

$$\tilde{A} = A + \sum_m \sum_n r_{mn} v_m^{(x)} v_n^{(y)}. \tag{54}$$

For an equi-spaced array in both the x and y directions,

$$v_m^{(x)} = w_m^{(x)} \exp(-imu),$$
$$v_n^{(y)} = w_n^{(y)} \exp(-inv), \quad (55)$$

where u and v are given by (22).

We restrict consideration to uncorrelated and equal-variance gain perturbations. Then (30) yields

$$|A|^2 = \left|\sum_m v_m^{(x)}\right|^2 \left|\sum_n v_n^{(y)}\right|^2 = \left|\sum_m w_m^{(x)} \exp(-imu)\right|^2 \left|\sum_n w_n^{(y)} \exp(-inv)\right|^2,$$

$$D = \sigma_r^2 \sum_m |v_m^{(x)}|^2 \sum_n |v_n^{(y)}|^2 = \sigma_r^2 \sum_m w_m^{(x)2} \sum_n w_n^{(y)2},$$

$$S = \sigma_r^2 \sum_m v_m^{(x)2} \sum_n v_n^{(y)2} = \sigma_r^2 \left[\sum_m w_m^{(x)2} \exp(-i2mu)\right]\left[\sum_n w_n^{(y)2} \exp(-in2v)\right]. \quad (56)$$

For the particular case of $\theta_\ell = \theta = 0$, (22) yields v = 0. Equation (56) then reveals results that are identical to the linear array, except that $|A|^2$ is scaled by $\left[\sum_n w_n^{(y)}\right]^2$, and D and S are scaled by $\sum_n w_n^{(y)2}$. That is, the line array results are directly applicable if a new effective element tolerance of σ_r^2/N_{eff} is used insead of σ_r^2, where

$$N_{eff} = \frac{\left[\sum_n w_n^{(y)}\right]^2}{\sum_n w_n^{(y)2}}. \quad (57)$$

Thus the extra dimension afforded by a planar array causes a smoothing effect on the random power response. This feature, shown here only for a particular slice in the u, v plane, will be shown later to be a general result; the (generally) increased number of elements in a planar array allows for more variation in the element gains.

For symmetric weights and M x N elements (M, N even), we find

$$A = \exp\left(-i\frac{M+1}{2}u - i\frac{N+1}{2}v\right) A_r^{(x)}(u) A_r^{(y)}(v),$$
$$D = \sigma_r^2 S_r^{(x)}(0) S_r^{(y)}(0),$$
$$S = \exp\left(-i(M+1)u - i(N+1)v\right) \sigma_r^2 S_r^{(x)}(u) S_r^{(y)}(v), \quad (58)$$

where real functions

$$A_r^{(x)}(u) \equiv 2 \sum_{m=1}^{M/2} w_m^{(x)} \cos\left(\frac{2m-M-1}{2} u\right),$$

$$S_r^{(x)}(u) \equiv 2 \sum_{m=1}^{M/2} w_m^{(x)^2} \cos\left((2m-M-1)u\right), \tag{59}$$

with corresponding definitions for real functions $A_r^{(y)}(v)$ and $S_r^{(y)}(v)$. Then (28) yields

$$E\{\tilde{P}\} = A_r^{(x)^2}(u)\, A_r^{(y)^2}(v),$$

$$\mathrm{Var}\{\tilde{P}\} = 2\sigma_r^2 A_r^{(x)^2}(u) A_r^{(y)^2}(v)\left[S_r^{(x)}(0) S_r^{(y)}(0) + S_r^{(x)}(u) S_r^{(y)}(v)\right]$$

$$+ \sigma_r^4 \left[S_r^{(x)^2}(0) S_r^{(y)^2}(0) + S_r^{(x)^2}(u) S_r^{(y)^2}(v)\right]. \tag{60}$$

Some useful properties of these functions are now listed: $A_r^{(x)^2}(u)$ has period 2π and is even in u; $A_r^{(y)^2}(v)$ has period 2π and is even in v; $S_r^{(x)}(u)$ has period 2π and is even in u; and $S_r^{(y)}(v)$ has period 2π and is even in v. Therefore we need compute (60) only for $0 \le u, v \le \pi$.

In figure 15, a 16 x 16 element array with multiplicative Dolph-Chebyshev weighting, designed for -30 dB side lobes in both x and y directions, is considered. In figure 15a, $\sigma_r^2 = 0.1$, whereas in figure 15b, $\sigma_r^2 = 0.01$; both results are for a slice along the v = 0 axis. It is seen that the element gain variability should be at least as small as that in figure 15b. In figures 15c-15e, the slices in the u, v plane are taken along the directions $v = \pi/8$, $v = u/4$, and $v = u$, respectively. The -60 dB level in the last figure for larger u is a result of the multiplicative weight patterns adopted. The average responses saturate near the -40 dB level in the deep side lobe region.

Results for an array of equal weights are given in figure 16, whereas multiplicative Hanning weighting is considered in figure 17. Both results are along the v = u slice in the u, v plane. The deep side lobes predicted by Hanning weighting are filled in, as figure 17 indicates. The pattern for a equi-weighted array is not affected as drastically.

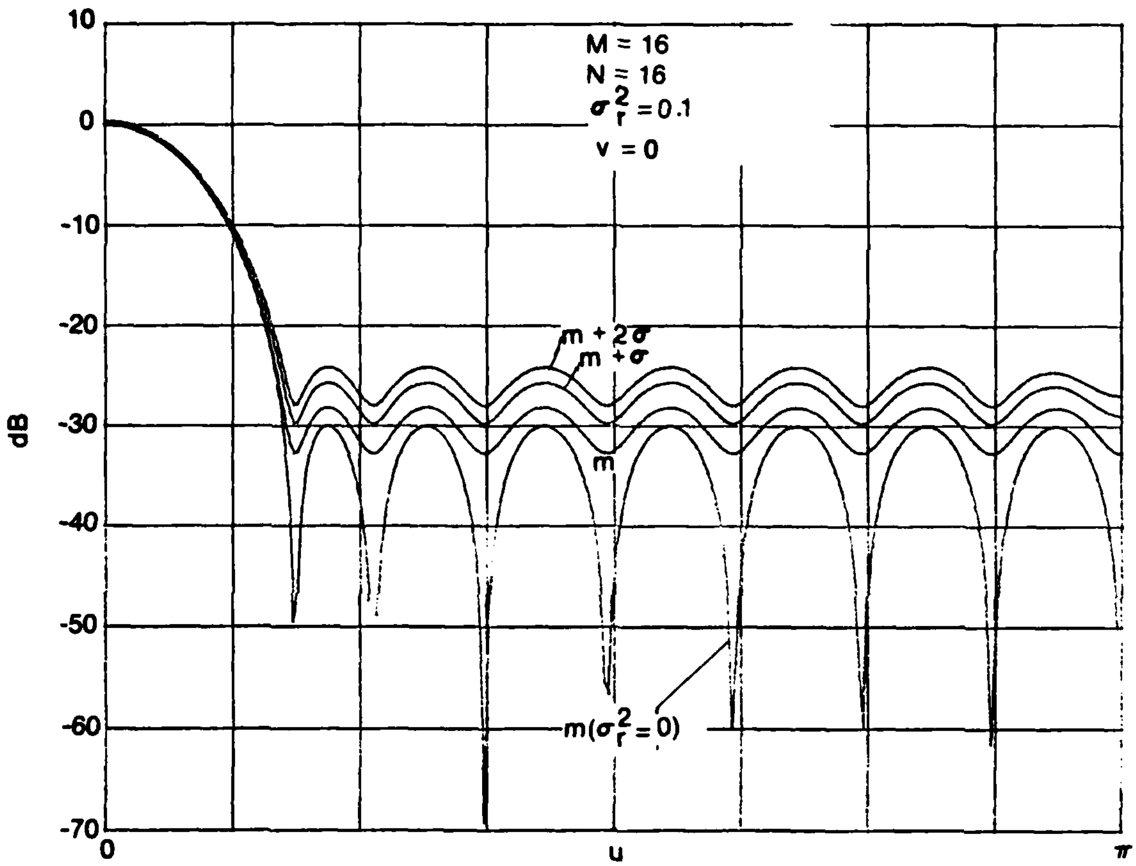

Figure 15a. Average Power Responses for Dolph-Chebyshev -30 dB Weighting; Planar Array; $\sigma_r^2 = 0.1$, v = 0

Figure 15. Average Power Responses for Dolph-Chebyshev -30 dB Weighting; Planar Array

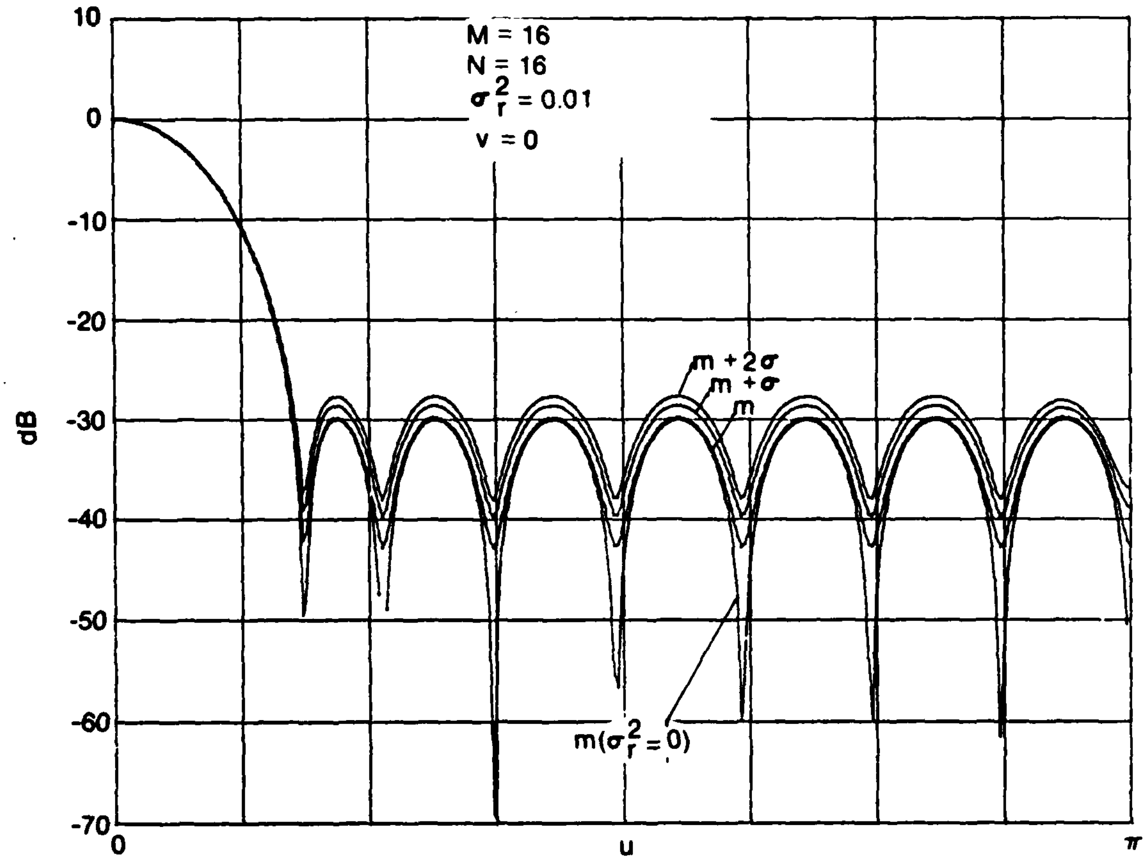

Figure 15b. Average Power Responses for Dolph-Chebyshev -30 dB Weighting; Planar Array; σ_r^2 = 0.01, v = 0

Figure 15. (Cont'd) Average Power Responses for Dolph-Chebyshev -30 dB Weighting; Planar Array

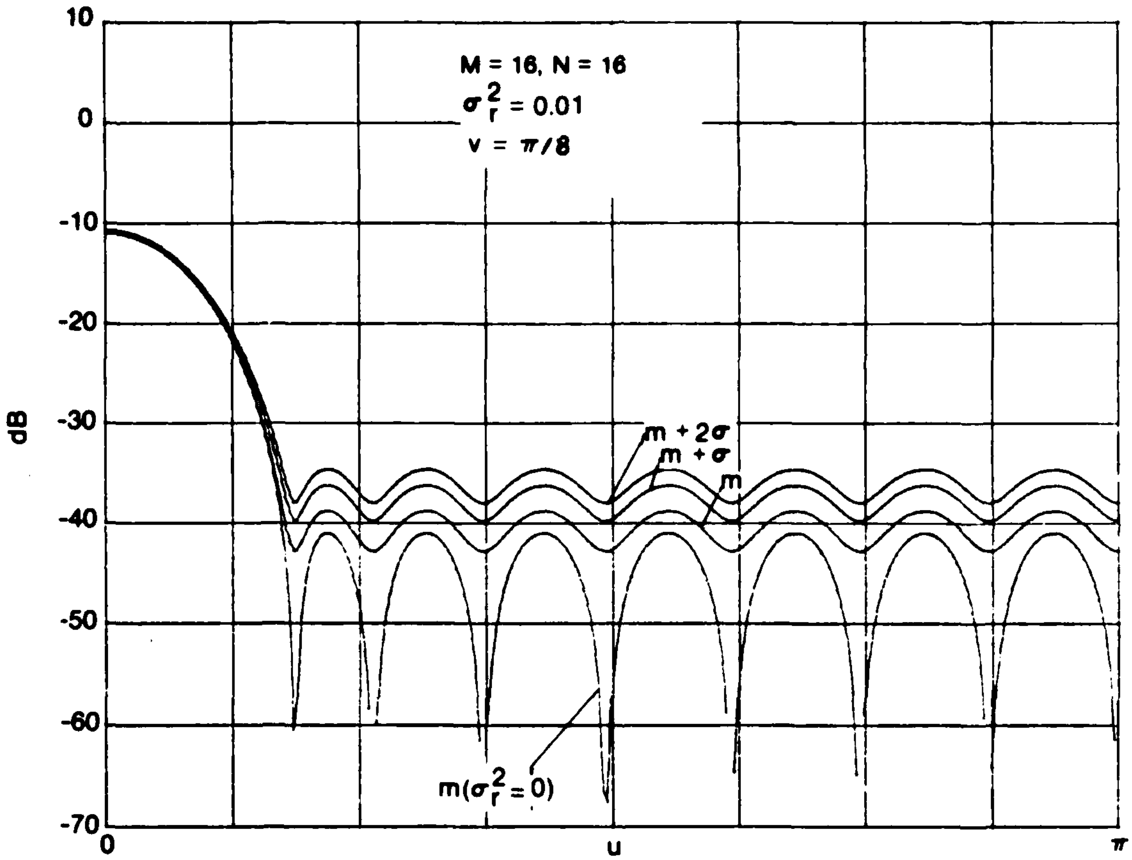

Figure 15c. Average Power Responses for Dolph-Chebyshev -30 dB Weighting; Planar Array; $\sigma_r^2 = 0.01, v = \pi/8$

Figure 15. (Cont'd) Average Power Responses for Dolph-Chebyshev -30 dB Weighting; Planar Array

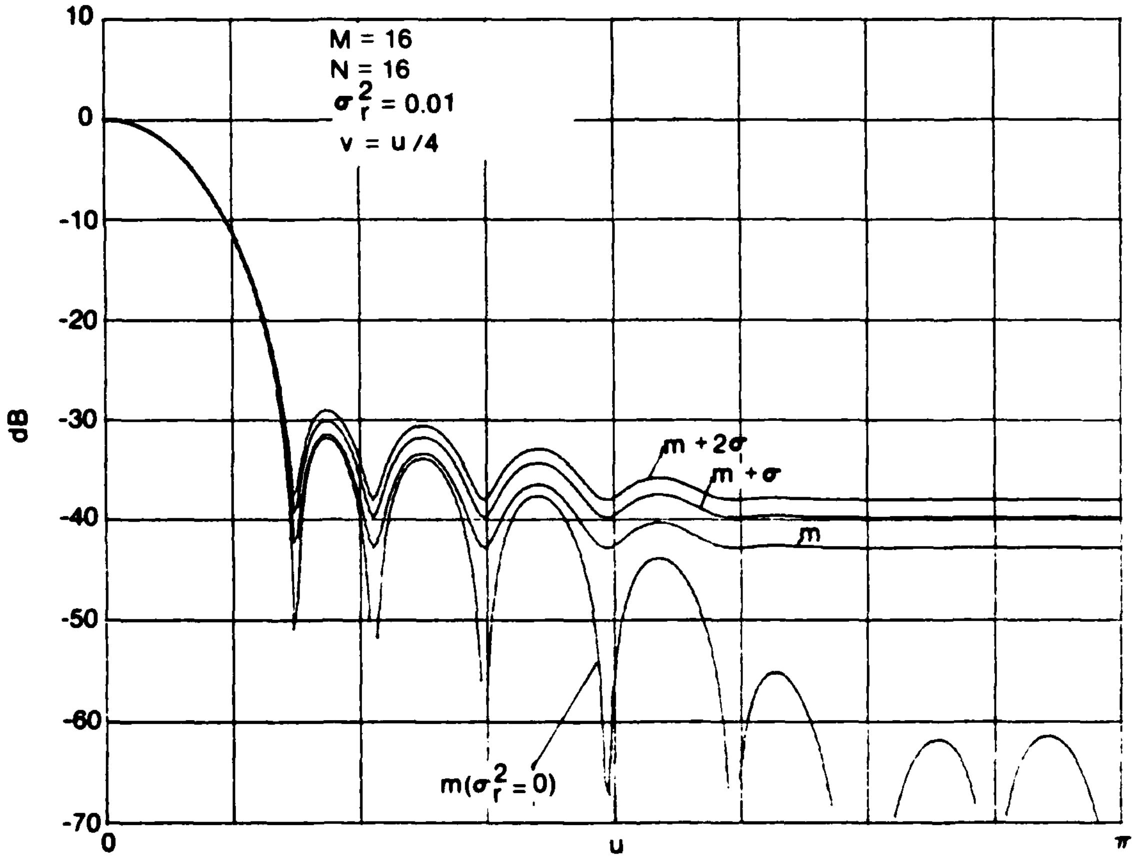

Figure 15d. Average Power Responses for Dolph-Chebyshev -30 dB Weighting; Planar Array; $\sigma_r^2 = 0.01, v = u/4$

Figure 15. (Cont'd) Average Power Responses for Dolph-Chebyshev -30 dB Weighting; Planar Array

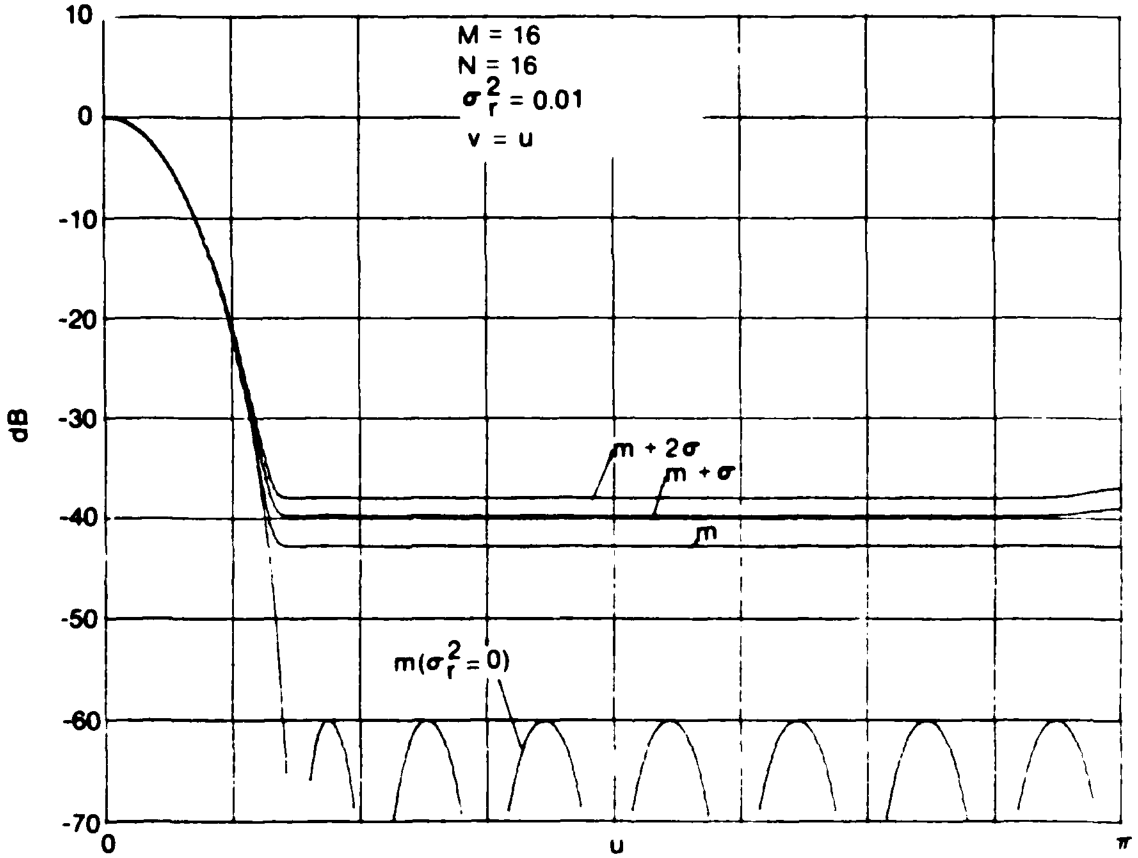

Figure 15e. Average Power Responses for Dolph-Chebyshev -30 dB Weighting; Planar Array; $\sigma_r^2 = 0.01$, v = u

Figure 15. (Cont'd) Average Power Responses for Dolph-Chebyshev -30 dB Weighting; Planar Array

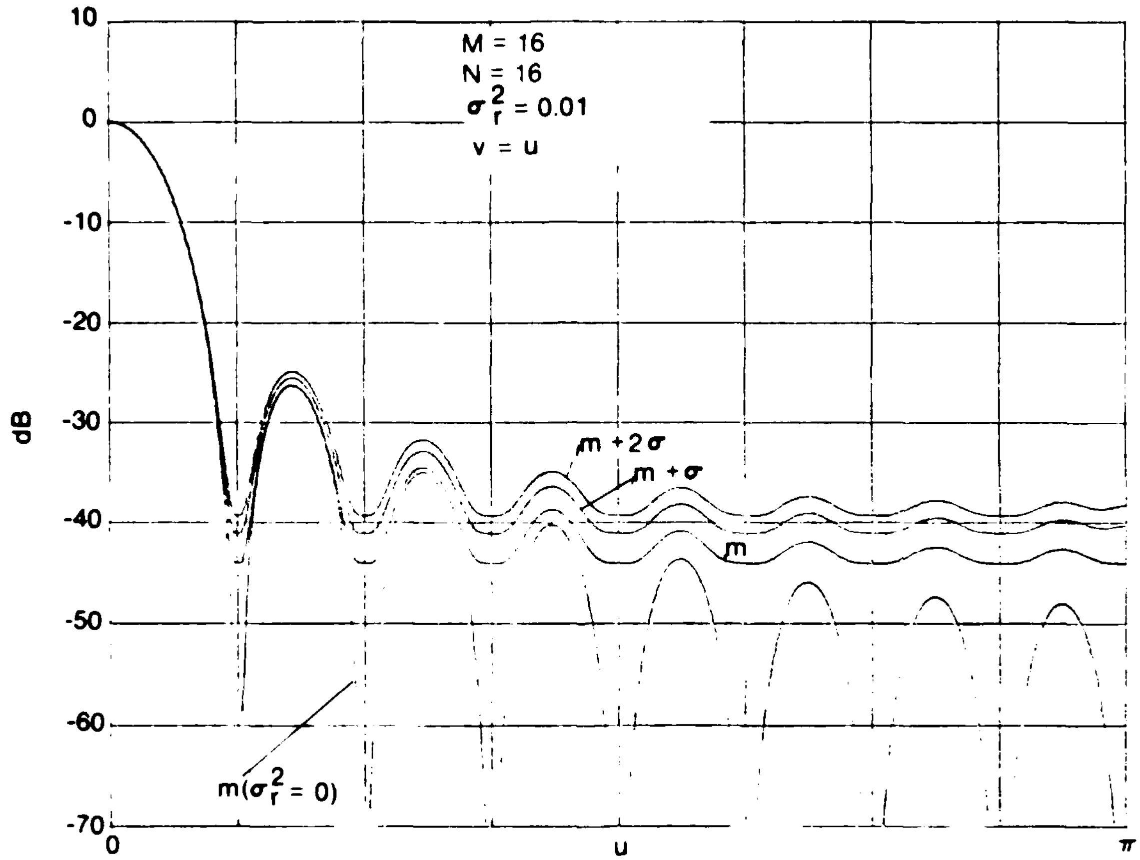

Figure 16. Average Power Responses for Equal Weighting; Planar Array

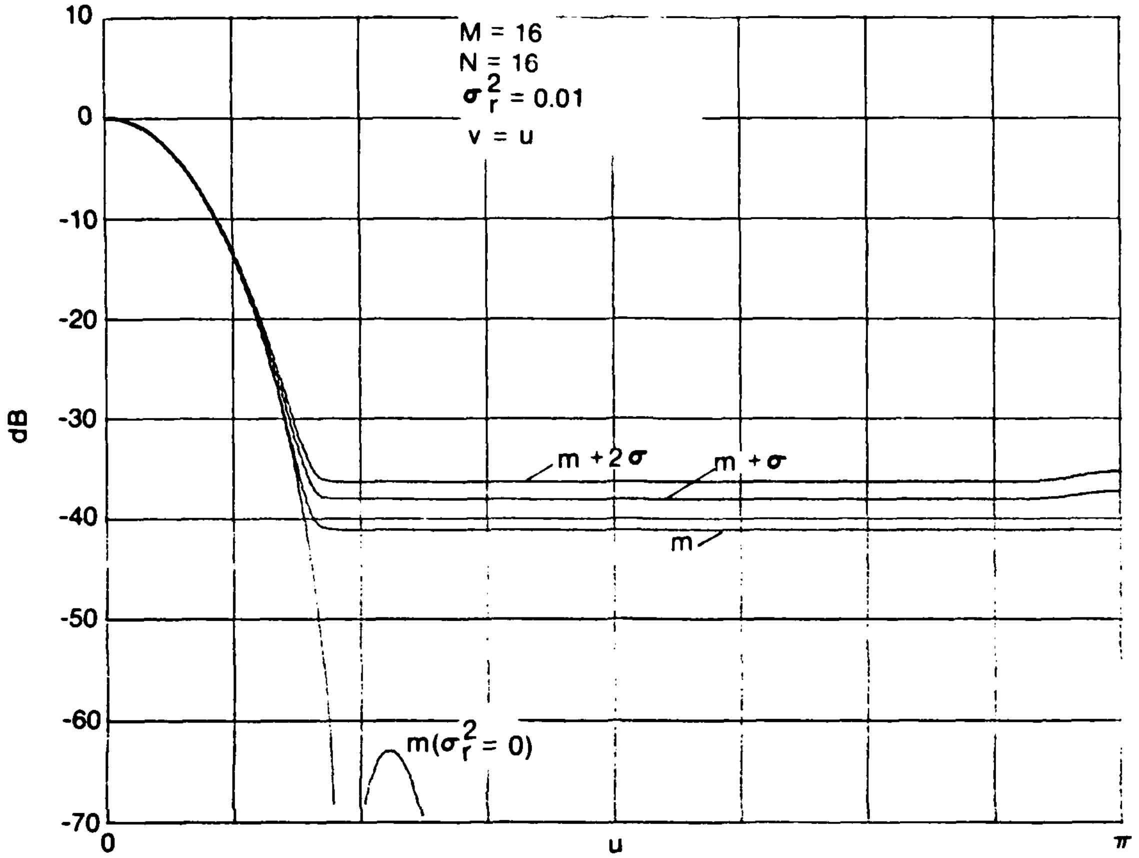

Figure 17. Average Power Responses for Hanning Weighting; Planar Array

Just as for the linear array, a simple expression for the saturation level in the deep side lobe region may be obtained. From (25), for a general array,

$$\tilde{P} = \left| A + \sum_k r_k v_k \right|^2 . \tag{61}$$

In the deep side lobe region, $|A|$ goes to zero and we have

$$\tilde{P} \cong \left| \sum_k r_k v_k \right|^2 = \sum_k \sum_\ell r_k r_\ell v_k v_\ell^* , \tag{62}$$

giving

$$E\{\tilde{P}\} = \sum_k \sum_\ell \sigma_{k\ell}^2 v_k v_\ell^* . \tag{63}$$

For uncorrelated equal-variance gain perturbations, (63) simplifies to

$$E\{\tilde{P}\} = \sigma_r^2 \sum_k |v_k|^2 = \sigma_r^2 \sum_k w_k^2 . \tag{64}$$

Therefore, for $w_k \geq 0$, the saturation level for the mean power response, relative to the peak response (for $\sigma_r = 0$), is

$$\frac{E\{\tilde{P}\}}{|A|^2_{max}} = \sigma_r^2 \frac{\sum_k w_k^2}{\left(\sum_k w_k\right)^2} \equiv \frac{\sigma_r^2}{K_{eff}} . \tag{65}$$

This result applies to an arbitrary array, not necessarily planar.

For a planar array, as described earlier,

$$K_{eff} = \frac{\left(\sum_m \sum_n w_{mn}\right)^2}{\sum_m \sum_n w_{mn}^2} , \tag{66}$$

and if the weights are multiplicative (see (19)), then

$$K_{eff} = \frac{\left(\sum_m w_m^{(x)} \sum_n w_n^{(y)}\right)^2}{\sum_m w_m^{(x)2} \sum_n w_n^{(y)2}} = M_{eff} N_{eff} . \tag{67}$$

To deduce the variance of $\tilde{P}$ in the deep side lobe region, we use (62) to obtain

$$E\{\tilde{P}^2\} = \sum_k \sum_\ell \sum_m \sum_n \overline{r_k r_\ell r_m r_n} \; V_k V_\ell^* V_m V_n^* . \tag{68}$$

For Gaussian $\{r_k\}$ which are uncorrelated and of equal variance,

$$\overline{r_k r_\ell r_m r_n} = \sigma_r^4 \left(\delta_{k\ell} \delta_{mn} + \delta_{km} \delta_{\ell n} + \delta_{kn} \delta_{\ell m}\right). \tag{69}$$

When this result is employed in (68) and coupled with (64), there follows

$$\mathrm{Var}\{\tilde{P}\} = \sigma_r^4 \left[\left(\sum_k |V_k|^2\right)^2 + \left|\sum_k V_k^2\right|^2\right] . \tag{70}$$

In the deep side lobes, the second term of (70) is negligible, and we have

$$\text{Std. Dev.}\{\tilde{P}\} = \sigma_r^2 \sum_k |V_k|^2 = E\{\tilde{P}\} . \tag{71}$$

Thus $\sigma = m$, giving $m + k\sigma = m(1+k)$, and (51) and table 2 hold again. These results hold for arbitrary arrays with any weight structure. The two fundamental parameters governing behavior in the deep side lobe region are σ_r^2 and K_{eff} in (65).

SUMMARY

Results for the mean power response and the standard deviation of the power response of an array (linear or planar) have been derived for arbitrary multiplicative beamformer weighting. The degree of widening of the main lobe response caused by deep side lobe designs can be evaluated quantitatively. A simple rule of thumb for the saturation level in the deep side lobe region has been presented; it depends only on the relative variation of the individual element gains and on the effective number of elements in the array. Specifications of tolerances of element gain perturbations can be made quantitative once the array size and type of array pattern have been selected.

Appendix A

PROBABILITY DISTRIBUTION OF POWER RESPONSE

The power response is given in (25) and (7) as

$$\tilde{P} = \left| \sum_k (1+r_k) v_k \right|^2 = \left| A + x + iy \right|^2 = (A_r + x)^2 + (A_i + y)^2 , \tag{A-1}$$

where

$$x + iy \equiv \sum_k r_k v_k . \tag{A-2}$$

Now x and y are correlated zero-mean real Gaussian random variables. In particular, from (A-2) and (24),

$$E\left\{(x+iy)^2\right\} = E\left\{x^2 - y^2 + i2xy\right\} = \sum_k \sum_j \sigma_{kj}^2 v_k v_j \equiv S ,$$

$$E\left\{|x+iy|^2\right\} = E\left\{x^2 + y^2\right\} = \sum_k \sum_j \sigma_{kj}^2 v_k v_j^* \equiv D . \tag{A-3}$$

Therefore

$$E\left\{x^2\right\} = \frac{1}{2}\left(D + S_r\right) \equiv \sigma_x^2 ,$$

$$E\left\{y^2\right\} = \frac{1}{2}\left(D - S_r\right) \equiv \sigma_y^2 ,$$

$$E\left\{xy\right\} = \frac{1}{2} S_i \equiv \sigma_x \sigma_y \rho , \tag{A-4}$$

where subscripts r and i denote real and imaginary parts, respectively.

Then the probability that random variable $\tilde{P}$ is less than T^2 is given by (A-1) as

$$\mathrm{Prob}\left(\tilde{P} < T^2\right) = \mathrm{Prob}\left((A_r + x)^2 + (A_i + y)^2 < T^2\right)$$

$$= \mathrm{Prob}\left(\alpha^2 + \beta^2 < T^2\right) = \iint\limits_{\alpha^2+\beta^2<T^2} d\alpha\, d\beta\, p(\alpha, \beta), \tag{A-5}$$

where the probability density of the linearly transformed variables $\alpha = A_r + x$, $\beta = A_i + y$ is joint Gaussian:

$$p(\alpha,\beta) = \left(2\pi\sigma_x\sigma_y\sqrt{1-\rho^2}\right)^{-1} \exp\left[-\frac{\left(\frac{\alpha - A_r}{\sigma_x}\right)^2 + \left(\frac{\beta - A_i}{\sigma_y}\right)^2 - 2\rho\left(\frac{\alpha - A_r}{\sigma_x}\right)\left(\frac{\beta - A_i}{\sigma_y}\right)}{2\left(1-\rho^2\right)}\right] . \tag{A-6}$$

Thus (A-5) corresponds to integration of a bivariate elliptical normal density over a circle offset from its peak at $\alpha, \beta = A_r, A_i$. After rotating coordinates in (A-5) and (A-6) to obtain independent random variables, we can use the table in reference 1 to evaluate (A-5).

Appendix B

CHARACTERISTIC FUNCTION OF POWER RESPONSE

From (A-1) through (A-4), we have the power response

$$\tilde{P} = (A_r + x)^2 + (A_i + y)^2 \tag{B-1}$$

and the probability density

$$p(x,y) = \left(2\pi\sigma_x\sigma_y\sqrt{1-\rho^2}\right)^{-1} \exp\left[-\frac{(x/\sigma_x)^2 + (y/\sigma_y)^2 - 2\rho(x/\sigma_x)(y/\sigma_y)}{2(1-\rho^2)}\right] . \tag{B-2}$$

The characteristic function of $\tilde{P}$ is then

$$f(\xi) = E\left\{\exp(i\xi\tilde{P})\right\} = \iint dx\, dy\; p(x,y) \exp\left[i\xi\left\{(A_r+x)^2 + (A_i+y)^2\right\}\right]$$

$$= \left(2\pi\sigma_x\sigma_y\sqrt{1-\rho^2}\right)^{-1} \iint dx\, dy\, \exp\left[-\alpha x^2 - \beta y^2 + 2\gamma xy + \mu x + \nu y + i\xi|A|^2\right] , \tag{B-3}$$

where

$$\alpha = \left[2\sigma_x^2(1-\rho^2)\right]^{-1} - i\xi$$

$$\beta = \left[2\sigma_y^2(1-\rho^2)\right]^{-1} - i\xi$$

$$\gamma = \rho\left[2\sigma_x\sigma_y(1-\rho^2)\right]^{-1}$$

$$\mu = i\xi 2A_r$$

$$\nu = i\xi 2A_i \; . \tag{B-4}$$

Now (reference 4, 3.323 2)

$$\iint dx\, dy \exp\left[-\alpha x^2 - \beta y^2 + 2\gamma xy + \mu x + \nu y\right]$$

$$= \frac{\pi}{\sqrt{\alpha\beta - \gamma^2}} \exp\left[\frac{\beta\mu^2 + \alpha\nu^2 + 2\gamma\mu\nu}{4(\alpha\beta - \gamma^2)}\right], \alpha_r > 0, \beta_r > 0, \alpha_r\beta_r > \gamma_r^2. \tag{B-5}$$

All the conditions in (B-5) are satisfied since $\rho^2 \leq 1$: From (A-3),

$$|S| = \left|E\{(x+iy)^2\}\right| \leq E\{|x+iy|^2\} = D; \tag{B-6}$$

therefore, from (A-4) and (B-6),

$$\rho^2 = \frac{S_i^2}{D^2 - S_r^2} = \frac{S_i^2}{S_i^2 + (D^2 - |S|^2)} \leq 1. \tag{B-7}$$

Employing the definitions in (B-4), we have

$$\alpha\beta - \gamma^2 = \frac{1 - i\xi 2(\sigma_x^2 + \sigma_y^2) + (i\xi)^2 4\sigma_x^2\sigma_y^2(1-\rho^2)}{4\sigma_x^2\sigma_y^2(1-\rho^2)} \tag{B-8}$$

and

$$\beta\mu^2 + \alpha\nu^2 + 2\gamma\mu\nu = (i\xi)^2 4\left\{\frac{A_r^2\sigma_x^2 + A_i^2\sigma_y^2 + 2A_rA_i\sigma_x\sigma_y\rho}{2\sigma_x^2\sigma_y^2(1-\rho^2)} - i\xi|A|^2\right\}. \tag{B-9}$$

Combining (B-3), (B-5), (B-8), and (B-9), we can express the characteristic function of $\tilde{P}$ as

$$f(\xi) = \left[1 - i\xi 2(\sigma_x^2 + \sigma_y^2) + (i\xi)^2 4\sigma_x^2\sigma_y^2(1-\rho^2)\right]^{-1/2} \cdot$$

$$\exp\left[i\xi \frac{|A|^2 - i\xi 2(A_r^2\sigma_y^2 + A_i^2\sigma_x^2 - 2A_rA_i\sigma_x\sigma_y\rho)}{1 - i\xi 2(\sigma_x^2 + \sigma_y^2) + (i\xi)^2 4\sigma_x^2\sigma_y^2(1-\rho^2)}\right]. \tag{B-10}$$

Now, by eliminating variables in favor of the original quantities via (A-4), there follows

$$2\left(\sigma_x^2+\sigma_y^2\right)=2D$$

$$4\,\sigma_x^2\,\sigma_y^2\left(1-\rho^2\right)=D^2-|S|^2$$

$$2\left(A_r^2\sigma_y^2+A_i^2\sigma_x^2-2A_rA_i\sigma_x\sigma_y\rho\right)=|A|^2D-\mathrm{Re}\left\{A^2S^*\right\} \qquad \text{(B-11)}$$

and

$$f(\xi)=\left[1-i\xi 2D+(i\xi)^2\left(D^2-|S|^2\right)\right]^{-1/2}\exp\left[i\xi\,\frac{|A|^2-i\xi\left(|A|^2D-\mathrm{Re}\left\{A^2S^*\right\}\right)}{1-i\xi 2D+(i\xi)^2\left(D^2-|S|^2\right)}\right]. \qquad \text{(B-12)}$$

A single numerical Fourier transform in (B-12) would yield the probability distribution of $\tilde{P}$ (reference 2) for specified values of A, D, and S. We do not pursue that tack but, instead, derive the cumulants of $\tilde{P}$. In (B-12), we let

$$x=i\xi,\ a=2D,\ b=D^2-|S|^2,\ c=|A|^2,\ d=|A|^2D-\mathrm{Re}\left\{A^2S^*\right\}, \qquad \text{(B-13)}$$

where $a \geq 0$, $b \geq 0$, $c \geq 0$, $d \geq 0$, to obtain

$$f=\left[1-xa+x^2b\right]^{-1/2}\exp\left[x\,\frac{c-xd}{1-xa+x^2b}\right]. \qquad \text{(B-14)}$$

We then expand $\ln f$ in a power series in x,

$$\ln f=\sum_{m=1}^{\infty}c_m\frac{x^m}{m!}\ , \qquad \text{(B-15)}$$

obtaining the cumulants

$$c_m=m!\left(\tfrac{1}{2}R_m+c\,S_{m-1}-d\,S_{m-2}\right), \qquad \text{(B-16)}$$

where

$$R_m \equiv \sum_{k=0}^{[m/2]} \frac{(-1)^k}{m-k} \binom{m-k}{k} a^{m-2k} b^k , \quad m \geq 1,$$

$$S_m \equiv \sum_{k=0}^{[m/2]} (-1)^k \binom{m-k}{k} a^{m-2k} b^k , \quad m \geq 0. \tag{B-17}$$

In particular,

$$c_1 = \frac{1}{2} a + c$$

$$c_2 = \frac{1}{2} a^2 - b + 2ca - 2d$$

$$c_3 = a^3 - 3ab + 6c(a^2 - b) - 6da . \tag{B-18}$$

In terms of the original quantities, using (B-13),

$$c_1 = |A|^2 + D = E\{\tilde{P}\}$$

$$c_2 = D^2 + |S|^2 + 2D|A|^2 + 2\,\mathrm{Re}\{A^2 S^*\} = \mathrm{Var}\{\tilde{P}\}$$

$$c_3 = 2D^3 + 6D|S|^2 + 6D^2|A|^2 + 6|S|^2|A|^2 + 12D\,\mathrm{Re}\{A^2 S^*\}$$

$$= E\left\{\left(\tilde{P} - E\{\tilde{P}\}\right)^3\right\} . \tag{B-19}$$

The first relationship in (B-19) for the mean c_1 of $\tilde{P}$ actually holds for any distribution of $\{r_k\}$, not just Gaussian; this is most easily seen by direct use of (25), (24), (7), and (A-3).

Appendix C

MOMENTS OF POWER RESPONSE FOR NON-GAUSSIAN PERTURBATIONS

From (25) and (7), the power response is

$$\tilde{P} = \left| A + \sum_k r_k v_k \right|^2 . \tag{C-1}$$

The mean of $\tilde{P}$ was derived in (32) and is given by

$$E\{\tilde{P}\} = |A|^2 + m_2 \sum_k |v_k|^2 . \tag{C-2}$$

The mean square value of $\tilde{P}$ is available from (C-1), (31), and the independence of $\{r_k\}$, as follows:

$$\begin{aligned} E\{\tilde{P}^2\} &= E\Big\{\Big(A + \sum_k r_k v_k\Big)\Big(A^* + \sum_\ell r_\ell v_\ell^*\Big)\Big(A + \sum_m r_m v_m\Big)\Big(A^* + \sum_n r_n v_n^*\Big)\Big\} \\ &= |A|^4 + 4|A|^2 m_2 \sum_k |v_k|^2 + A^2 m_2 \sum_k v_k^{*2} + A^{*2} m_2 \sum_k v_k^2 \\ &\quad + 2A m_3 \sum_k |v_k|^2 v_k^* + 2A^* m_3 \sum_k |v_k|^2 v_k + \sum_{k\ell mn} E\{r_k r_\ell r_m r_n\} v_k v_\ell^* v_m v_n^* . \end{aligned} \tag{C-3}$$

The fourth-order average in (C-3) has the value m_4 if all four subscripts are identical, and the value m_2^2 if two of the subscripts are identical and the other two are identical, but not with the former pair. Then the last term in (C-3) is expressible as

$$\begin{aligned} & m_4 \sum_k |v_k|^4 + m_2^2 \Big[2 \sum_{\substack{k,m \\ k \neq m}} |v_k|^2 |v_m|^2 + \sum_{\substack{k,\ell \\ k \neq \ell}} v_k^2 v_\ell^{*2} \Big] \\ &= m_4 \sum_k |v_k|^4 + m_2^2 \Big[2 \Big(\sum_k |v_k|^2 \Big)^2 + \Big| \sum_k v_k^2 \Big|^2 - 3 \sum_k |v_k|^4 \Big] . \end{aligned} \tag{C-4}$$

Equation (C-3) then becomes

$$E\{\tilde{P}^2\} = |A|^4 + 4|A|^2 m_2 \sum_k |v_k|^2 + 2m_2 \,\mathrm{Re}\Big\{A^2 \sum_k v_k^{*2}\Big\}$$
$$+ 4m_3 \,\mathrm{Re}\Big\{A \sum_k |v_k|^2 v_k^*\Big\} + m_4 \sum_k |v_k|^4$$
$$+ m_2^2 \Big[2\Big(\sum_k |v_k|^2\Big)^2 + \Big|\sum_k v_k^2\Big|^2 - 3\sum_k |v_k|^4\Big]. \quad \text{(C-5)}$$

Combining this result with (C-2), there follows

$$\mathrm{Var}\{\tilde{P}\} = 2m_2\Big[|A|^2 \sum_k |v_k|^2 + \mathrm{Re}\Big\{A^2 \sum_k v_k^{*2}\Big\}\Big]$$
$$+ 4m_3 \,\mathrm{Re}\Big\{A \sum_k |v_k|^2 v_k^*\Big\}$$
$$+ m_2^2\Big[\Big(\sum_k |v_k|^2\Big)^2 + \Big|\sum_k v_k^2\Big|^2\Big] + \big(m_4 - 3m_2^2\big)\sum_k |v_k|^4. \quad \text{(C-6)}$$

Appendix D

ELEMENT GAIN PERTURBATIONS EXPRESSED IN DECIBELS

The voltage gain of the k-th element was given in (23), (7), and (8) as

$$(1 + r_k) w_k \equiv e_k \,. \tag{D-1}$$

Then (for $w_k > 0$) the probability

$$\text{Prob}(e_k < V) = \text{Prob}(w_k(1+r_k) < V) = \text{Prob}\left(r_k < \frac{V}{w_k} - 1\right) = P_k\left(\frac{V}{w_k} - 1\right), \tag{D-2}$$

where P_k is the cumulative distribution function of random variable r_k.

Choose voltage levels V_U, V_L such that

$$\begin{aligned} \text{Prob}(e_k < V_U) &= T_U \quad (= 0.9 \text{ e.g.}), \\ \text{Prob}(e_k < V_L) &= T_L \quad (= 0.1 \text{ e.g.}) . \end{aligned} \tag{D-3}$$

That is,

$$P_k\left(\frac{V_{U,L}}{w_k} - 1\right) = T_{U,L} \;, \tag{D-4}$$

or voltage levels

$$V_{U,L} = w_k\left(1 + P_k^{-1}(T_{U,L})\right). \tag{D-5}$$

These are the voltage levels within which element voltage gain e_k can be found with tail probabilities T_L, $1 - T_U$.

We now define decibel levels (corresponding to the specified probability values $T_{U,L}$), relative to the design value w_k, as

$$dB_{U,L} \equiv 20 \log\left(\frac{V_{U,L}}{w_k}\right) = 20 \log\left(1 + P_k^{-1}(T_{U,L})\right) \qquad \text{(D-6)}$$

The range (dB_L, dB_U) is that range within which the element gain perturbations can be found with tail probabilities T_L, $1 - T_U$. (We get the same result if we consider the power gain e_k^2 as the fundamental random variable, provided that $r_k > -1$, $w_k > 0$.) If $\mathrm{Var}(r_k) = 0$, then

$$P_k(x) = \begin{Bmatrix} 1, & x \geq 0 \\ 0, & x < 0 \end{Bmatrix}$$

$$P_k^{-1}(y) = 0 \text{ for } 0 < y < 1, \qquad \text{(D-7)}$$

and $dB_{U,L} = 0$, as expected.

For Gaussian element perturbations,

$$P_k(x) = \Phi\left(\frac{x}{\sigma_k}\right), \qquad \text{(D-8)}$$

where Φ is the Gaussian cumulative distribution function:

$$\Phi(t) = \int_{-\infty}^{t} du\, (2\pi)^{-1/2} \exp(-u^2/2). \qquad \text{(D-9)}$$

Then (D-6) yields

$$dB_{U,L} = 20 \log\left(1 + \sigma_k \Phi^{-1}(T_{U,L})\right), \qquad \text{(D-10)}$$

where Φ^{-1} is the inverse Φ function.

For uniform element perturbations,

$$P_k(x) = \frac{x}{2\sqrt{3}\,\sigma_k} + \frac{1}{2}, \quad |x| < \sqrt{3}\,\sigma_k,$$

$$P_k^{-1}(y) = 2\sqrt{3}\,\sigma_k\left(y - \tfrac{1}{2}\right), \quad 0 < y < 1. \qquad \text{(D-11)}$$

Then (D-6) yields

$$dB_{v,i} = 20 \log\left(1 + 2\sqrt{3}\,\sigma_k\left(T_{v,i} - \frac{1}{2}\right)\right). \tag{D-12}$$

Equations (D-10) and (D-12) are plotted in figures 3 and 4, respectively.

REFERENCES

1. G. W. Rosenthal and J. J. Rodden, "Tables of the Integral of the Elliptical Bivariate Normal Distribution Over Offset Circles," Lockheed Missiles and Space Division, Sunnyvale, CA, LMSD-800619, 1 May 1961.

2. A. H. Nuttall, Alternate Forms and Computational Considerations for Numerical Evaluation of Cumulative Probability Distributions Directly From Characteristic Functions, NUSC Technical Report 3012, 12 August 1970.

3. C. L. Dolph, "A Current Distribution for Broadside Arrays Which Optimizes the Relationship Between Beamwidth and Side Lobe Level," Proc. IRE, vol. 34, June 1946, pp. 335-348.

4. I. S. Gradshetyn and I. M. Ryzhik, Table of Integrals, Series, and Products, Academic Press, New York, NY, 1965.

DATE
ILMED
-8